SRESA's International Journal of

LIFE CYCLE RELIABILITY AND SAFETY ENGINEERING

Vol.3 **Issue No.2** **April–June 2014** **ISSN – 2250 0820**

Special Issue :

On

"Extended Version of Selected Papers from SMiRT-21"

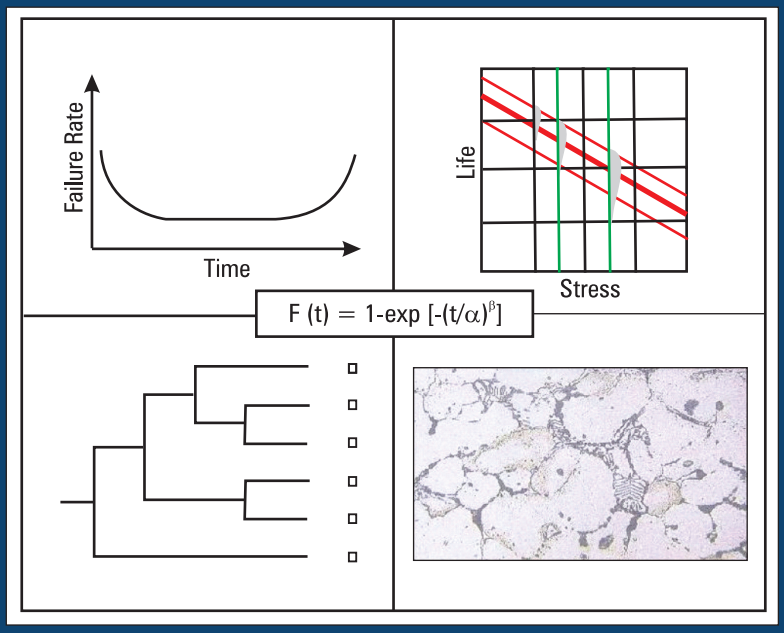

Guest-Editors
Dr. B. K. Dutta
Dr. R. K. Singh

Chief-Editors
P.V. Varde
A.K. Verma
Michael G. Pecht

Society for Reliability and Safety
website: http://www.sresa.org.in

SRESA Journal of Life Cycle Reliability and Safety Engineering

Extensive work is being performed world over on assessment of Reliability and Safety for engineering systems in support of decisions. The increasing number of risk-based / risk-informed applications being developed world over is a testimony to the growth of this field. Here, along with probabilistic methods, deterministic methods including Physics-of-Failure based approach is playing an important role. The International Journal of Life Cycle Reliability and Safety Engineering provides a unique medium for researchers and academicians to contribute articles based on their R&D work, applied work and review work, in the area of Reliability, Safety and related fields. Articles based on technology development will also be published as Technical Notes. Review articles on Books published in the subject area of the journal will also form part of the publication.

Society for Reliability and Safety has been actively working for developing means and methods for improving system reliability. Publications of quarterly News Letters and this journal are some of the areas the society is vigorously pursuing for societal benefits. Manuscript in the subject areas can be communicated to the Chief Editors. Manuscript will be reviewed by the experts in the respective area of the work and comments will be communicated to the corresponding author. The reviewed final manuscript will be published and the author will be communicated the publication details. Instruction for preparing the manuscript has been given on inside page of the end cover page of each issue. The rights of publication rest with the Chief-Editors.

SCOPE OF JOURNAL

System Reliability analysis	**Structural Reliability**	**Risk-based applications**
Statistical tools and methods	Remaining life prediction	Technical specification optimization
Probabilistic Safety Assessment	Reliability based design	Risk-informed approach
Quantitative methods	Physics-of-Failure methods	Risk-based ISI
Human factor modeling	Probabilistic Fracture Mechanics	Risk-based maintenance
Common Cause Failure analysis	Passive system reliability	Risk-monitor
Life testing methods	Precursor event analysis	Prognostics & health management
Software reliability	Bayesian modeling	Severe accident management
Uncertainty modeling	Artificial intelligence in risk and reliability modeling	Risk-based Operator support systems
Dynamic reliability models	Design of Experiments	Role of risk-based approach in Regulatory reviews
Sensitivity analysis	Fuzzy approach in risk analysis	Advanced electronic systems reliability modeling
Decision support systems	Cognitive framework	Risk-informed asset management

SRESA AND ITS OBJECTIVES

a) To promote and develop the science of reliability and safety.

b) To encourage research in the area of reliability and safety engineering technology & allied fields.

c) To hold meetings for presentation and discussion of scientific and technical issues related to safety and reliability.

d) To evolve a unified standard code of practice in safety and reliability engineering for assurance of quality based professional engineering services.

e) To publish journals, books, reports and other information, alone or in collaboration with other organizations, and to disseminate information, knowledge and practice of ensuring quality services in the field of Reliability and Safety.

f) To organize reliability and safety engineering courses and / or services for any kind of energy systems like nuclear and thermal power plants, research reactors, other nuclear and radiation facilities, conventional process and chemical industries.

g) To co-operate with government agencies, educational institutions and research oganisations

SRESA's International Journal of

LIFE CYCLE RELIABILITY AND SAFETY ENGINEERING

Vol.3 Issue No.2 April–June 2014 ISSN – 2250 0820

Special Issue :

On

"Extended Version of Selected Papers from SMiRT-21"

Guest-Editors

Dr. B. K. Dutta
Dr. R. K. Singh

Chief-Editors

P.V. Varde
A.K. Verma
Michael G. Pecht

SOCIETY FOR RELIABILITY AND SAFETY

Typeset & Printed

EBENEZER PRINTING HOUSE
Unit No. 5 & 11, 2nd Floor, Hind Services Industries,
Veer Savarkar Marg,
Dadar (west), Mumbai -28
Tel.: 2446 2632/ 3872
E-mail: outwork@gmail.com

Editorial

This special issue highlights the important and extended versions of contributions made in SMiRT 21 to knowledge base of structural reliability and safety.

This issue contains 5 papers. The first 4 papers are extended versions of selected papers from SMiRT 21. All these papers are in the area of 'Structural Reliability', which is in the scope of this journal. The 5th paper is a regular paper that also falls under structural reliability.

The first paper is about the safety factor evaluation for prestressed inner containment shell in Indian NPPs. The paper concentrates on development of partial safety factors (PSF) for accidental pressure design. PSFs account for uncertainties in load, material and mathematical modeling. The paper develops a set of optimal reliability-based PSFs for the design of prestressed concrete at collapse limit state under MSLB/LOCA conditions.

The second paper evaluates failure probability of expansion bellow at reactor containment building. A computationally efficient evaluation method – Higher Order Response surface method – has been used for the evaluation. The method uses Chebyshev polynomial for estimation of order of stochastic variables. The method also facilitates the sensitivity analysis without any additional computational cost.

The third paper is about seismic fragility analysis of nuclear reactor SSCs (Structures, Systems and components). The paper reports the results of seismic re-evaluation of an operating reactor FBTR (Fast Breeder Test Reactor). The objectives of this re-evaluation are – safe shutdown of the plant, maintenance of safe shutdown, long-term decay heat removal and containment of radioactivity. The paper details out the probabilistic seismic hazard analysis to determine seismic demand, safety analysis to identify SSCs and different approaches adopted in the seismic fragility analysis.

The fourth paper is about updating the reliability models of structures using measure responses. The challenges involved in the process are determination of system parameters/forcing functions followed by solution of a constrained non-linear optimization problem – inverse reliability. The solution methods used in the paper are application of Bayes' theorem, subset simulation and numerical optimization.

The fifth paper describes safety assessment of NPP pipelines against thermomechanical fatigue in presence of hybrid uncertainities. For piping components in high temperature applications, theromomechanical fatigue is one of the primary life-limiting factors. The paper employs a strain-based approach for safety assessment. A case study has been taken to illustrate their method.

We sincerely hope that this special issue will provide a stimulating experience to all our valued readers.

Dr. B.K. Dutta
Dr. R.K. Singh

Prof B. K. Dutta, *is a Distinguished Scientist and Senior Professor, Dean of Homi Bhabha National Institute and Heading Human Resource Development Division & Structural and Material Mechanics Section of Reactor Safety Division at Bhabha Atomic Research Centre, Mumbai. He is a member of the 'Governing Council of Atomic Energy Education Society, Member, International Association for SMiRT and Member Secretary of 'Council of Management and 'Academic Council' of HBNI. He pioneered work in the area of reactor structural safety. The work pursued him involves development of basic formulations, development of new computer codes, solutions of complex reactor problems, accomplishment of Five-year plan projects, implementation of academic programs and human resource development. He has got more than two hundred and seventy five technical publications including seventy-seven papers in peer reviewed journals. His Publications have more than 650 citations with h factor 12. He is also author of a book-chapter published by WIT press (UK). He is guest editor of two special issues of 'Indian Journal SADHNA' and 'International Journal on Nuclear Engineering Design'. He is the inaugural recipient of Technical Excellence Award (1992) and Homi Bhabha Award for Science and Technology (1997) of Department of Atomic Energy. He is a fellow of Indian National Academy of Engineering.*

Dr. Ram Kumar Singh, *is a Distinguished Scientist, Head of Reactor Safety Division at Bhabha Atomic Research Centre, Mumbai and Senior Professor Homi Bhabha National Institute.*

Dr Singh is an active researcher with over 36 years of experience and has been involved in finite element code development for coupled fluid-structure-thermal interaction problems for reactor safety issues, experimental stress analysis, nuclear containment structural and thermal hydraulics safety studies, impact and high strain rate problems for soft and hard missiles. His recent focus has been on tsunami evaluation of Indian coastal nuclear facilities, containment integrity, hydrogen transport and combustion for reactor safety assessment and development of severe accident management guidelines for Indian nuclear power plants and facilities. At present as Head Reactor Safety Division at BARC Trombay, he supervises a team of 70 nuclear engineers who are responsible for structural mechanics, thermal hydraulics, reliability and safety evaluation of Indian nuclear reactors for design and beyond design basis accidents for external and internal extreme events, which are addressed through plan projects and collaboration with academic and research institutes.

He Worked under Hydrogen Economy Program as Guest Scientist in Institute of Nuclear and Energy Technology (IKET) Forschungszentrum (FZK) Karlsruhe, Germany (2003-04).

Dr. R K Singh has guided a large number of Ph D and M Tech students at IITs/IISc and Homi Bhabha National Institute. Dr Singh served as Chairman of International Scientific Committee for 21st International Conference on Structural Mechanics in Reactor Technology (SMiRT-21), and has been the guest editor of the Special Issue of Nuclear Engineering and Design on Selected Papers of SMiRT 21, (Vol. 269, April-2014). He has organized a number of international and national conferences and has successfully coordinated standard problem and round robin exercises on concurrent computational mechanics / experimental studies related to reactor safety problems.

Dr Singh is a fellow of Indian National Academy of Engineering and member of Indian Nuclear Society, Indian Association for Computational Mechanics and Indian Society for Heat and Mass Transfer. He is recipient of Homi Bhabha Science and Technology Award -2011 for his distinguished contributions.

He has published 65 papers in International Journals, 5 Books, 210 papers in International Conferences and 114 papers in National Conferences.

Life Cycle Reliability and Safety Engineering
Vol.3 Issue 2 (2014) 1-14

Development of Partial Safety Factors for Accidental Pressure Design Case of Prestressed Inner Containment Shells in Indian NPPS

Baidurya Bhattacharya[1], Aritra Chatterjee[1], Gunjan Agrawal[2], Apurba Mondal[3]
[1]*Indian Institute of Technology Kharagpur, Kharagpur, India*
[2]*ZS Associates, Pune, India*
[3] *Nuclear Power Corporation of India Ltd., Mumbai, India*
E-mail: baidurya@civil.iitkgp.ernet.in

Abstract

Partial safety factors (PSFs) used in reliability-based design are intended to account for uncertainties in load, material and mathematical modeling while ensuring that the target reliability is satisfied for the relevant class of structural components in the given load combination and limit state. This paper describes the methodology in detail for developing a set of optimal reliability-based PSFs for the design of prestressed concrete inner containment shells in Indian NPPs at collapse limit state under MSLB/LOCA conditions. The mechanical formulation of the flexural limit state is based on the principle behind prestressed concrete design recommended by IS 1343 and SP16. The applied biaxial moments are combined according to Wood's criteria. The optimization of the PSFs is based on reliability indices obtained from importance sampling and a local linear response surface fit; Monte Carlo simulations are performed to determine the capacity statistics and dependence between capacity and applied loads. Numerical examples are provided.

Keywords: Reliability, partial safety factor, optimization, prestressed concrete shell, nuclear power plant

1. Introduction

The design of containment shells for Indian Pressurized Heavy Water Reactors (PHWRs) has evolved over the years, originating from a steel cylindrical shell capped with a steel dome (CIRUS Reactor, Trombay), followed by the use of reinforced concrete walls and pre-stressed concrete dome (Rajasthan Atomic Power Station) to the use of Pre-Stressed concrete for the entire shell (Madras Atomic Power Station) and pre-stressed concrete double containment shells (first employed in the Narora and Kakrapar Power Stations). The Kaiga and Rajasthan Atomic Power Plants marked a further improvement in the design philosophy with complete double containment shells having independent domes [1]. The inner containment shells used in recent PHWRs are cylindrical structures of 63 m height, with prestressed concrete spherical domes containing 4 large openings to facilitate the replacement of steam generators. [2]. Until recently, nuclear containment structures in India were designed using the French RCC-G code. The raft of the PWHR at Tarapur was designed using the ASME code and checked against RCC-G [1]. There is yet no formal Indian design standard for containment structures. In 2007, the Atomic Energy Regulatory Board (AERB) of India released the CSE-3 codes [3] which is currently under review.

Significant uncertainties exist in the structural behavior of the IC Shells of PHWRs, arising out of the random nature of material, geometry, prestressing and loadings. As early as 1974, Shinozuka and Shao [4] conducted a probabilistic assessment of prestressed concrete pressure vessels using the first order second moment approximation. Uncertainties in loads and in the material and geometry of the vessels were considered while short term accidental load effects were modeled as Poisson Processes. The overall uncertainty in structural behavior of nuclear containment structures, as in any general structure, is caused by uncertainties in resistance and demand quantities. The uncertainty associated with the resistance of containment shells arises out of uncertainty in the strengths of concrete and steel as well as in shell geometry. While concrete strength has been found to be better controlled in the nuclear power plant industry than in the ordinary building industry, steel strength variability does not display a noticeable reduction. Variability in sectional dimensions is comparatively quite low and has negligible impact on the overall uncertainty in structural resistance [5].

Loads acting on concrete containments intrinsically involve random uncertainties, and therefore need to be treated probabilistically. Different loads have different degrees of randomness and may entail appropriate adjustments in the probabilistic framework, for example, the variability of dead load being substantially lower than that of an accidental pressurization load, the former can be treated as a deterministic quantity for simplification of analysis [6]. Another significant source of uncertainty is the long term behavior of these structures which is highly variable owing to material changes (for example, prestress loss in tendons and creep in concrete) and the occurrence of accidental events [7, 8].

It is most rational to treat uncertainties associated with parameters governing the design and construction of a structure in a probabilistic format, specifically, to model the time-invariant quantities as random variables and the time-dependent ones as stochastic processes. Recognizing the existence of these uncertainties is an admission of the fact that the structure may not always satisfy its performance and safety objectives during its intended design life. The logical extension of this admission is to ensure that the likelihood of unsatisfactory performance be kept acceptably low during the life of the structure.

The subject of structural reliability provides the tools and methodologies to explicitly determine the probability of such failures ("failure" here in the sense of non-compliance or non-performance) by taking into account all relevant uncertainties. These techniques can be used to design new structures with specified (i.e., target) reliabilities, and to maintain existing structures at or above specified reliabilities. Target reliabilities are discussed in the next subsection. Even though such computed probabilities of failure (reliability being 1 minus failure probability) may not have a frequentist or actuarial basis, structural reliability provides a neutral and non-denominational basis to compare different (and often disparate) designs and maintenance strategies on a common basis.

A limit state function (or performance function), $g(\underline{X})$, for a structural component is defined in terms of the basic variables, $\underline{X}$, such that:

$$\begin{aligned} g(\underline{X}) &< 0 \text{ denotes failure} \\ g(\underline{X}) &> 0 \text{ denotes satisfactory performance} \end{aligned} \quad (1)$$

and the surface given by:

$$g(\underline{X}) = 0 \quad (2)$$

is called the limit state equation or limit state surface. The performance function g is typically obtained from the mechanics of the problem at hand. For multiple failure modes or if there are multiple critical sections, Eq. is generalized to an appropriate union of failure events.

The basic variable generally comprise of quantities like material properties, loads or load-effects, environmental parameters, geometric quantities, modeling uncertainties, etc. They are usually modeled as random variables; however, those with negligible `uncertainties may be treated as deterministic. The general expression of failure probability is

$$P_f = P\left(g(\underline{X}) < 0\right) = \int_{g(\underline{x})<0} f_{\underline{X}}(\underline{x}) d\underline{x} \quad (3)$$

where $f_X(x)$ is the joint probability density function for $\underline{X}$. The reliability of the structure would then be defined as $Rel = 1 - P_f$.

Like any other design approach, reliability based design is an iterative process: the design is adjusted until adequate safety is achieved and cost and functional requirements are met. The final step of meeting the target reliability can either be direct where the computed structural reliability has to exactly satisfy the target reliability for each relevant limit state or it can be indirect as in partial safety factors (PSF) based design where the structure implicitly satisfies the target reliability within a certain tolerance [9]. The term load and resistance factor design (LRFD) implies the approach followed in the United States where the nominal resistance in the design equation is multiplied by an explicit "resistance factor" but the nominal material properties that go into determining the resistance are not factored. The term PSF based design implies the approach taken in Europe where there is no explicit resistance factor in design, but each material property generally has its own partial safety factor. The latter approach is taken in this work.

Closed-form solutions to Eq. are generally unavailable. Two different approaches are widely in use: (i) analytic methods based on constrained optimization and normal probability approximations, and (ii) simulation based algorithms with or without variation reduction techniques and both can provide accurate and efficient solutions to the structural reliability problem. The first kind, grouped under First Order Reliability Methods (or FORM), holds an advantage over the simulation based methods in that

the design point(s) and the sensitivity of each basic variable can be explicitly determined. However, FORM can prove to be costly or even infeasible if the size of the reliability problem goes up (in terms of basic variables and/or number of limit states) or if the limit state is not analytic in the basic variables, and is not used in this work. Monte Carlo simulations with Importance Sampling have been used to compute failure probabilities.

2. Target Reliability

It has become increasingly common to express safety requirements, as well as some functionality requirements, in reliability based formats. A reliability based approach to design, by accounting for randomness in the different design variables and uncertainties in the mathematical models, provides tools for ensuring that the performance requirements are violated as rarely as considered acceptable.

The cause, reference period, and consequences of violation of different performance requirements may vary, and if a reliability approach is taken, the target reliability in each performance requirement must take such difference into account [9-12]. For example, If the structure gives appropriate warning before collapse, the failure consequences reduce and that in turn can reduce the target reliability for that mode [11, 13]. Functionality target reliabilities may be developed exclusively from economic considerations. The safety target reliability levels required of a structure, on the other hand, cannot be left solely to the discretion of the owner, or be derived solely from a minimum total expected cost consideration, since structural collapse causing a large loss of human life and/or property may not be acceptable either to the society or the regulators. Design codes, therefore often place a lower limit on the reliability of safety related limit states [9, 14]. For optimizing a structure with multiple performance requirements, Wen [15] suggested minimizing the weighted sum of the squared difference of the target and actual reliabilities.

ISO 2394 [10], and later JCSS [11], proposed three levels of requirements with appropriate degrees of reliability: (i) serviceability (adequate performance under all expected actions), (ii) ultimate (ability to withstand extreme and/or frequently repeated actions during construction and anticipated use), (iii) structural integrity (i.e., progressive collapse in ISO 2394 and robustness in JCSS). Target reliability values were suggested based on the consequences of failure for ultimate limit states and relative cost of safety measure for serviceability limit states. The Canadian Standards Association [16] defines two safety classes and one serviceability class (and corresponding annual target reliabilities) for the verification of the safety of offshore structures (i) Safety class 1- great risk to life or high potential for environmental pollution or damage, 2) Safety class 2-small risk to life or low potential for environmental pollution or damage, and 3) Serviceability Impaired function and none of the other two safety classes being violated. Det Norske Veritas [13] specifies three types of structural failures for offshore structures and target reliabilities for each corresponding to the seriousness of the consequences of failure. The American Bureau of Shipping [17] identified four levels of failure consequences for various combinations of limit states and component class for the concept Mobile Offshore Base and assigned target reliabilities for each. Ghosn & Moses [18] suggest three levels of performance to ensure adequate redundancy of bridge structures corresponding to functionality, ultimate and damaged condition limit states, while Nowak et al. [19] recommend two different reliability levels for bridge structures corresponding to ultimate and serviceability limit states. Nuclear power plant containment structures are designed for earthquakes at two different levels of intensity and correspondingly to two different criteria for failure [3, 20, 21]. Damage, if any, caused by the Operating Basis Earthquake (OBE) must not lead to loss of functionality of the nuclear power plant; whereas the Safe Shutdown Earthquake (SSE) that has a higher intensity and longer recurrence interval than OBE, is allowed to cause the power plant to shut down but must not cause any radioactive leakage to the environment or loss of structural integrity.

The fact that the consequences of failure of a critical component in a nuclear reactor are potentially catastrophic has driven the interest in building so called "inherently safe reactors" which are publicly perceived to have a zero probability of failure. The application of a probabilistic risk assessment framework to such structures then has the dual purpose of determining the probability of meeting the stipulated conditions under which "inherently safe" performance is guaranteed, and the probability of departure from acceptable performance under these conditions. Values of maximum acceptable probability levels set by regulatory authorities of different nations for accidents that cause severe damage to the reactor core have ranged from $1x10^{-6}$ per year to $1x10^{-4}$ per year [22].

Given the inability to predict the occurrence or magnitude of earthquakes, the uncertainties involved from source to site, and the potential for massive damage, it is not surprising that performance based design has been most enthusiastically espoused in the seismic engineering community, as evident in SEAOC [23], ATC-40 [24] and FEMA 273/274 [25]. Performance levels for seismic design are commonly defined in terms of increasing severities, e.g., (i) Immediate Occupancy (IO), the state of damage at which the building is safe to occupy without any significant repairs, (ii) Structural Damage (SD), an intermediate level of damage in which significant structural and non-structural damage has occurred without loss of global stability, and (iii) Collapse Prevention (CP), representing extensive structural damage that causes global instability [26]. A comparison of the performance of structures designed to one ultimate design earthquake vs. those designed to dual level performance levels indicated that the latter produces relatively stronger structures [15]. A similar finding was echoed by Ghobarah [27] who opined that the reason for the revision of the then design standards to more reliable performance based methods was that after severe earthquakes (such as Northridge and Kobe), while structures designed to the existing codes performed well with respect to safety, the extent of damage and the economic costs were unexpectedly high.

3. Reliability of Prestressed Concrete Sections

The tensile strength of concrete is negligible compared to its compressive strength. In ordinary reinforced concrete, the reinforcing steel is used to carry the tensile stresses, and the concrete near the tensile face may crack. Prestressing is intended to artificially induce compressive stresses in the concrete to counteract the tensile stresses caused by external loads, such that the loaded section remains mostly if not entirely in compression [28].

Prestressed concrete (for shells, slabs, girders etc.) is often adopted when in addition to satisfying strength requirements, the member is also required to be slender (e.g., from aesthetic or weight considerations) and/or to limit cracking (e.g., to satisfy leak-tightness). Prestressed concrete members are relatively lightweight as they are built from high strength steel and high strength concrete, more resistant to shear, and can recover from effects of overloading. However, prestressed concrete structures are more expensive, have a smaller margin for error, and the design process of prestressed members is more complicated. Although the loss of prestress with time is built into the design, unintended loss of prestress arising from corrosion of the tendons, slippage etc. can have catastrophic consequences.

Prestressed concrete sections may fail in several possible ways (such as a combination of flexure, shear and torsion, bursting of end blocks, bearing, anchorage or connection failures, excessive deflections etc.). This work however, only looks at ultimate flexural limit state defined by collapse of concrete due to crushing.

Several reliability based studies on partially prestressed concrete sections have been conducted in the past. Al-Harthy and Frangopol [29] studied prestressed beams designed to the 1989 ACI 318, considering 3 different limit states (ultimate flexure, cracking in flexure and permissible stresses), random dead and live loads, material and geometric properties, prestressing forces and modeling uncertainty. Their studies concluded that the reliability indices implied by the 1989 ACI 318 design standard are non-uniform over various ranges of loads, span lengths and limit states. Hamann and Bulleit [30] examined the reliability of under reinforced high-strength concrete prestressed beams designed in accordance with the 1983 ACI-318 standard, considering only the ultimate flexural limit state of beams subjected to dead and snow loads. While Al-Harthy and Frangopol included all the material and geometric random variables in a FORM analysis, Hamann and Bulleit first estimated the moment capacity through Monte Carlo simulations, fitted the data to standard distributions, and then performed a first order second moment reliability analysis on the linear limit state.

Reliability for Class-1 structures, particularly concrete containment structures for nuclear power plants, is a much researched subject primarily due to the dire failure consequences of the containment structure in terms of environmental impact, radiation effect on human health and other economic costs. Hwang et al. [6] described a Load and Resistance Factor Design (LRFD)-based approach to determine the critical load combinations for design of concrete containment structures. The limit state, corresponding to ultimate strength of concrete, was defined in the 2-D space of membrane stress and bending moment in the shell, leading to an octagonal limit state surface. Pandey [8] and Varpasuo [31] also worked on the

on the reliability of concrete containments, their limit states forming sides of the octagonal limit state considered by Hwang et al [6].

4. Mechanics of Pre-Stressed Concrete Sections

In this work, we look at collapse limit state of partially prestressed sections in flexure which corresponds to crushing of concrete in compression (reinforcements may yield). Bidirectional flexure on shell elements corresponding to nuclear power plant inner containment structures with voids have been modeled using Wood's criteria [32] summarized in Appendix A. The material properties of concrete and steel and the mechanistic formulation of both the limit states are discussed next.

In Indian Standards such as IS 456 [33] the compressive stress-strain relationship for concrete is taken to be parabolic up to a strain of 0.002, and horizontal from that point on. The nominal compressive strength of concrete is taken to be $f_{cn} = f_{ck}/1.5$ where f_{ck} is the characteristic compressive strength. The design compressive strength of concrete is f_{cn}/γ_c, where γ_c is the material safety factor on concrete strength. The value of γ_c is usually taken to be 1.5 for normal design condition and as 1.15 for abnormal design condition. The failure strain of concrete in bending compression is 0.0035. IS 1343[34] specifies the minimum grade of concrete as M30 for post-tensioning and M40 for pre-tensioning.

The stress-strain behavior of concrete in tension is linear [35] and the tensile strength is taken to be $f_{c\gamma} = 0.7\sqrt{f_{ck}}$ and the modulus of elasticity of concrete in tension is assumed to be same as the secant modulus of concrete in compression which is $E_c = 5000\sqrt{f_{ck}}$ The maximum tensile strain in concrete is then,

$$\varepsilon_{t\max} = \frac{f_{cr}}{E_c} = 0.00012 \qquad (4)$$

The design yield stress for reinforcing steel is f_{yn}/γ_s where f_{yn} is the nominal yield strength and γ_s is the material safety factor on yield strength of steel and is taken to be 1.15 for normal design conditions and 1.0 for abnormal conditions. The nominal modulus of elasticity of steel, E_n, is 200000 N/mm^2.

The moment capacity of a partially prestressed concrete section, given the amount of prestressing force and the geometric and material properties can be obtained in the form of an interaction diagram using strain compatibility equations and force balance. Interaction diagrams are plots of normalized compressive force, $P' = P/(f_{ck}bD)$ and normalized moment capacity, $M' = M/(f_{ck}bD^2)$ where b and D are the width and the depth of the section, respectively.

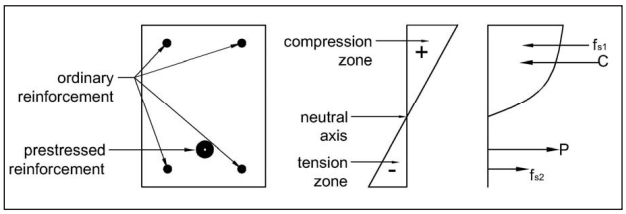

Fig.1: Force balance and moment computations for partially prestressed section

Figure 1 shows the strain and stress diagrams for an example section similar to the ones used in this work - with one set of prestressing tendons and two layers of ordinary reinforcement. In the figure, C= compressive force in concrete, f_{s1} = force in top reinforcement, f_{s2} = force in bottom reinforcement and P = prestressing force.

For given amount of prestress the position of the neutral axis is determined iteratively by balancing the tensile and compressive forces on the section. The moment capacity can then be found by taking the moment of the forces about any convenient point. In determining the collapse moment capacity, two cases are possible (Figure 2): the neutral axis (NA) outside and the neutral axis inside the section. In the former, the entire section is in compression and in the latter, concrete has cracked and is assumed not to carry any load in the tensile zone.

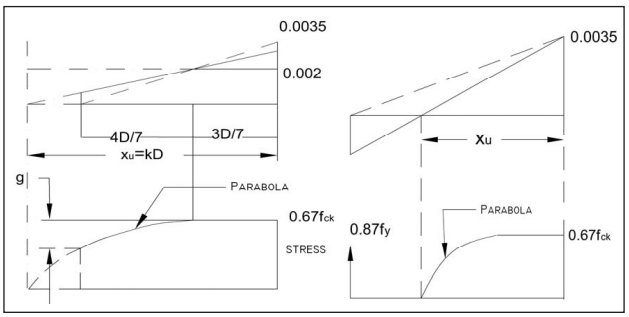

Fig.2: Strain and stress distributions on section for neutral axis outside (left) and inside (right) the section for limit state of collapse

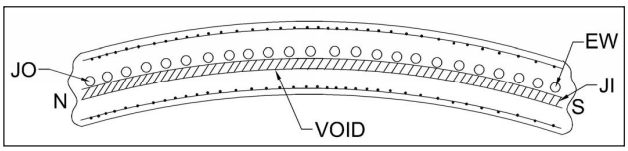

Fig.3: Prestressed concrete shell

Figure 3 shows an example prestressed concrete element corresponding to the shell structure of nuclear power plant inner containment structures. Two layers of ordinary reinforcement top and bottom can be seen and JI and JO correspond to prestressing cables in the North-South and East-West directions respectively. In the co-ordinate system adopted, these two are considered as the x and y directions.

When calculating the flexural strength of an element such as this, the space taken by the prestressing cable JI has to be considered as a void in concrete, i.e. while calculating the contribution of concrete to the strength the area considered is the total area minus the area of the void. For the typical prestressed containment shell, the void depth is approximately 0.15 times the total depth of the element.

The forces and moments acting on the section (for example Dead Load, Ordinary Live Load, Construction Live Load, Pre Stressing Load and Accidental Pressure Load) have two normal components (xx and yy) and one shearing (xy) component. Additionally, areas occupied by pre stressing cables are considered as voids in concrete. The section is thus under bi-directional flexural loading.

The components of the externally applied loads (N_{xx} and N_{yy}) on the section act in the same direction as the pre-stressing cables. As a result, the external forces cause the section to be in compression, thus acting like a external pre stressing forces. These forces therefore affect the moment capacity of the section. On the other end, applied moments on the section are caused due to the same set of forces. Thus both the capacity of the system and the loading on the system are affected by a common source and therefore it is possible that the applied moment and the moment capacity will show some degree of correlation.

The design check is carried out in the principal plane with respect to stresses. Applied moments are converted to this plane according to the basic rules of tensorial transformation. The moment capacities of the section in each of the 2 principal directions are computed from interaction diagrams with transformed dimensions, reinforcement areas and voids. The applied moments in directions X and Y are obtained using Wood's Criteria [32], summarized in Appendix A) which outlines a procedure to obtain applied moments in x and y direction at the bottom and the top of the section (M^*_{xtop}, $M^*_{xbottom}$, M^*_{ytop}, $M^*_{ybottom}$), eliminating the torsional moment component M_{xy}.

Since the structural analysis used to compute stress resultants is completely linear in nature, the different stress resultant components (N_{xx}, N_{yy}, N_{xy}, M_{xx}, M_{xy}, M_{xy}) in a given load case are statistically fully dependent on one another. Additionally, stress resultants due to different load cases are completely independent. The correlation matrix that is developed for analysis is based on these two assumptions.

5. Reliability Analysis and Calibration of PSFs

5.1 Limit States and Basic Variables

Since this work concerns the reliability of PC shells in biaxial flexure, the limit states in x and y directions can be written respectively as:

$$g_x = M_{\text{cap},x} - M_{\text{app},y} = 0 \tag{5}$$

$$g_y = M_{\text{cap},y} - M_{\text{app},y} = 0 \tag{6}$$

so that failure of the section is given by:

$$\{\text{Failure}\} = g_x < 0 \cup g_y < 0 \tag{7}$$

and the failure probability can be written as:

$$P_f = \int_{\underline{x}\in\{\text{Failure}\}} f_{\underline{X}}(\underline{x})\, d\underline{x} = \int_{\text{all } \underline{x}} \mathbf{I}\left[\{\text{Failure}\}\right] f_{\underline{X}}(\underline{x})\, d\underline{x} \tag{8}$$

The indicator function, **I**, on the right hand side of Eq. [4.4] evaluates the expression within brackets so that:

$$\mathbf{I}[\bullet] = \begin{cases} 1, \text{ if } [\bullet] \text{ is true} \\ 0, \text{ if } [\bullet] \text{ is false} \end{cases} \tag{9}$$

and is a convenient way to convert the domain of integration from the failure region to the entire range of $\underline{x}$ which is useful in simulation based estimates as described subsequently.

$M_{\text{cap},x}$ and $M_{\text{cap,y}}$ are the moment capacities in x and y directions respectively. Likewise, $M_{\text{app},x}$ and $M_{\text{app,y}}$ are the applied moments. As stated above, the moment capacity corresponds to collapse of the section. From this point forward, unless otherwise mentioned, all moments in this work are normalized by $f_{ck}bD^2$ and all forces by $f_{ck}bD$.

Before going into the details of the individual terms above, it is important to recall that the moment capacities and applied moments are mutually statistically dependent since the capacities are functions of the axial loads which in turn are linearly related to the applied moments in each load case. In addition, the capacities in the x and y directions

are strongly correlated as they are functions of the same material properties and some of the same axial loads.

As explained in Appendix-A, $M_{\text{app},x}$ and $M_{\text{app,y}}$ are defined respectively as $\max(\text{abs}(M^*_{xtop}), \text{abs}(M^*_{xbottom}))$ and $\max(\text{abs}(M^*_{ytop}), \text{abs}(M^*_{ybottom}))$ and are functions of the applied moments M_{xx} ,M_{yy} and M_{xy} caused by all load cases relevant to the load combination at hand. For example, we can have the load combination Dead (D) + Prestressing (P_s) + Ordinary Live (L_o) + Temperature (T) + Accidental Pressure (P_a) giving us:

$$\left.\begin{aligned} M_{xx} &= M_{xx,D} + M_{xx,Ps} + M_{xx,Lo} + M_{xx,T} + M_{xx,Pa} \\ M_{yy} &= M_{yy,D} + M_{yy,Ps} + M_{yy,Lo} + M_{yy,T} + M_{yy,Pa} \\ M_{xy} &= M_{xy,D} + M_{xy,Ps} + M_{xy,Lo} + M_{xy,T} + M_{xy,Pa} \end{aligned}\right\} \quad (10)$$

The normalized moment capacity, M_{cap}, is a function of the applied in-plane compression, material properties ($f_c, f_y, E, \varepsilon_c, \varepsilon_t$) and geometric quantities ($p/f_{ck}, d/D, e/D, t_{void}/D$):

$$M_{cap} = M_{\text{cap}}\left(P, f_c, f_y, E, \varepsilon_c, \varepsilon_t, \frac{p}{f_{ck}}, \frac{d}{D}, \frac{e}{D}, \frac{t_{void}}{D}\right) \quad (11)$$

Of these, the random terms are: the applied in-plane compressive force, P , the compressive strength of concrete, f_c , the yield strength, f_y , and the Young's modulus, E, of the reinforcing steel. The compressive force P in turn is the algebraic sum of forces from all load cases in the load combination considered.

The nominal or design values of the moment capacities, to be used in design equations discussed below, can be obtained by substituting the random quantities in Eq. [4.9] by their design values:

$$M_{cap,n} == M_{\text{cap}}\left(P_n, \frac{f_{cd}}{\gamma_c}, \frac{f_{yn}}{\gamma_s}, E_n, \varepsilon_c, \varepsilon_t, \frac{p}{f_{ck}}, \frac{d}{D}, \frac{e}{D}, \frac{t_{void}}{D}\right) \quad (12)$$

As stated above, in accidental pressure load case, the material safety factor on concrete compressive strength, γ_c is commonly taken to be 1.15, while that on yield strength of reinforcing steel, γ_s is commonly 1.0.

The moment capacities $M_{cap,x}$ and $M_{cap,y}$ thus defined are implicit functions of four basic variables; their distributions and correlations with applied moments are obtained by numerical simulation, which in turn are used in the reliability analyses.

5.2 Monte Carlo Simulations and Importance Sampling

Except in very special situations, closed form solution to the structural reliability problem (Eq.(8)) does not exist and numerical approximations are needed. The true probability of failure, P_f ,

$$P_f = \int_{\text{all } \underline{x}} \mathbf{I}\left[\{\text{Failure}\}\right] f_{\underline{X}}(\underline{x})\, d\underline{x} = \int_{\text{all } \underline{u}} \mathbf{I}\left[\{\text{Failure}\}\right] f_{\underline{U}}(\underline{u})\, d\underline{u} \quad (13)$$

can be estimated using basic (or "brute-force" or "crude") Monte Carlo simulations (MCS) in practice as:

$$\hat{P}_f = \frac{1}{N}\sum_{i=1}^{N} \mathbf{I}\left[g_x\left(T\left(\underline{U}_i\right)\right) < 0 \cup g_y\left(T\left(\underline{U}_i\right)\right) < 0\right] \quad (14)$$

where a zero-mean normal vector $\underline{U}$ with the same correlation matrix $\boldsymbol{\rho}$ as the basic variables is generated first and then transformed element by element according to the full distribution transformation:

$$T(\underline{u}) = \underline{x} \;\Rightarrow F_{X_i}(x_i) = \Phi(u_i) \quad (15)$$

The use of the same $\boldsymbol{\rho}$ for $\underline{U}$ as for $\underline{X}$ results in error, but the error is generally small [36]. N is the total number of times the random vector $\underline{U}$ is generated, and $\underline{U}_i$ is the i^{th} realization of the vector. It is well-known that the basic Monte-Carlo simulation-based estimate of P_f has a relatively slow and inefficient rate of convergence. The coefficient of variation (COV) of the estimate is:

$$\text{c.o.v.}(\hat{P}_f) = \sqrt{(1-P_f)/(NP_f)} \approx \sqrt{1/(NP_f)} \quad (16)$$

which is proportional to $1/\sqrt{N}$ and points to an inefficient relation between sample size and accuracy (and stability) of the estimate.

Such limitations of the basic Monte Carlo simulation technique have led to several "variance reducing" refinements. Notable among them is Latin hypercube sampling (e.g., [37]), importance sampling (e.g.[38]) along with its variants (e.g., [39], [40]) which, if performed carefully, can significantly reduce the required sampling size. Nevertheless, importance sampling and other variance reducing techniques should be performed with care, as their results may be quite sensitive to the type and the point of maximum likelihood of the sampling distribution, and an improper choice can produce erroneous results.. In this work, we have adopted Importance Sampling to estimate the failure probability in Eq.

The mathematical formulation of importance sampling is simply obtained by modifying the basic expression of failure probability (Eq.) as:

$$P_f = \int_{\underline{x}\in\{\text{Failure}\}} f_{\underline{X}}(\underline{x})d\underline{x} = \int_{\underline{x}\in\{\text{Failure}\}} \frac{f_{\underline{X}}(\underline{x})}{f_{\underline{H}}(\underline{x})} f_{\underline{H}}(\underline{x})d\underline{x} \qquad (17)$$

where $f_{\underline{H}}$ is any PDF not equal to zero in the region of interest. A judicious choice of $f_{\underline{H}}$ can ensure low variance of the estimated failure probability. By a simple change of the variable of integration, the failure probability estimate is as before the computation of the expectation of the indicator function but now modified with a correction factor ($f_{\underline{U}} / f_{\underline{H}}$):

$$\hat{P}_f = \frac{1}{N}\sum_{i=1}^{N} \mathrm{I}\left[g_x\left(T(\underline{h}_i)\right)<0 \cup g_y\left(T(\underline{h}_i)\right)<0\right] \frac{f_{\underline{U}}(\underline{h}_i)}{f_{\underline{H}}(\underline{h}_i)} \qquad (18)$$

It is important to note that this expectation as computed with respect to the sampling density $f_{\underline{H}}$ and the estimate of failure probability is obtained by simulating vectors of $\underline{H}$. The choice of $f_{\underline{H}}$ is extremely important, and depending on the limit state function, an improper choice may lead to errors in the estimate of P_f.

In this work, $\underline{H}$ has been taken as a jointly Normal random vector with the same correlation matrix **ρ** as $\underline{U}$, but with a mean vector that is closer to the failure region. This mean vector is chosen carefully by comparing the IS results with basic MCS results for the range of problems encountered. The variance of the estimate in Eq. (18) is:

$$\mathrm{var}(\hat{P}_f) = \frac{1}{N^2}\sum \mathrm{var}\left(\mathbf{I}_i \frac{f_{\underline{U}}(\underline{h}_i)}{f_{\underline{H}}(\underline{h}_i)}\right) \qquad (19)$$

which can be estimated during the sampling as:

$$\hat{S}^2(\hat{P}_f) = \frac{\sum \mathbf{I}^2 f_U^2 / f_H^2}{N^3} - \frac{1}{N^2}\left(\frac{\sum \mathbf{I} f_U / f_H}{N}\right)^2 \qquad (20)$$

giving the coefficient of variation (COV) of the failure probability estimated through importance sampling as:

$$\hat{V}(\hat{P}_f) = \frac{\hat{S}(\hat{P}_f)}{\hat{P}_f} \qquad (21)$$

One of our stopping criteria for the Importance Sampling simulation in this work involves an upper limit on the COV of the estimated failure probability.

5.3 Partial Safety Factors and their Optimization

Reliability based partial safety factor (PSF) design is intended to ensure a nearly uniform level of reliability across a given category of structural components for a given class of limit state under a particular load combination [41]. We approach the topic of optimizing PSFs by noting that any arbitrary point, $\underline{X}^a$, on the limit state surface by definition satisfies:

$$g(\underline{X}^a) = 0 \qquad (22)$$

Conversely, a "design point" $\underline{X}^d$ on the limit state surface can be carefully chosen so that it "locates" the limit state in the space of basic variables such that a pre-defined target reliability is ensured for the design. The ensuing design equation:

$$g(\underline{X}^d) = 0 \qquad (23)$$

is essentially a relationship among the parameters of the basic variables and gives a minimum requirement type of tool in the hand of the design engineer to ensure target reliability for the design in an indirect manner. Since nominal or characteristic values of basic variables are typically used in design, Eq. may be rewritten as:

$$g\left(\frac{X_1^n}{\gamma_1},...,\frac{X_k^n}{\gamma_k},\gamma_{k+1}X_{k+1}^n,...,\gamma_m X_m^n\right) \geq 0, \quad \text{where} \quad \frac{X_k^n}{\gamma_k} = X_k^d \qquad (24)$$

where the superscript n indicates the nominal value of the variable. We have partitioned the vector of basic variables into k resistance type and $m - k$ action type quantities. The partial safety factors, γ_i , are typically greater than one: for resistance type variables they divide the nominal values while for action type variables they multiply the nominal values to obtain the design point:

$$\begin{aligned} &\text{resistance PSFs}: \gamma_i = \frac{X_{i,n}}{X_i^d}, i = 1,...,k \\ &\text{action PSFs}: \gamma_i = \frac{X_i^d}{X_{i,n}}, i = k+1,...,m \end{aligned} \qquad (25)$$

If the design equation (23) can be separated into a strength term and a combination of load-effect terms, the following safety checking scheme may be adopted for design:

$$R_n\left(\frac{S_i^n}{\gamma_i^s}, i = 1,...,k\right) \geq l\left(\sum_{i=1}^{m-k}\gamma_i^q Q_i^n\right) \qquad (26)$$

where R_n = the nominal resistance and a function of factored strength parameters, l = load-effect function,

Table 1: Statistics of Basic Variables

Random Variable	Description	Statistics Distribution(mean, COV)	Source
$M'_{LC,xx}$ $M'_{LC,xy}$ $M'_{LC,yy}$	normalized applied moments	for each load case (LC) in given load combination, combined according to Wood's criteria	FEM Analysis of IC Shell Model
$P'_{LC,xx}$ $P'_{LC,xy}$ $P'_{LC,yy}$	normalized force	for each load case (LC) in given load combination	FEM Analysis of IC Shell Model
$M'_{cap,xx}$ $M'_{cap,yy}$	normalized moment capacity	obtained through Interaction diagram (fn of $P'_{LC,xx}$, $P'_{LC,xy}$ and $P'_{LC,yy}$)	Structural Analysis of Prestressed concrete section
f_c	compressive strength of concrete	Normal, (max(f_{ck}+0.825s_c, f_{ck}+4), s_c)*	[33]
f_y	Yield strength of steel	Lognormal(1.1133f_{yn},0.09)	[43], [30]
E	Young's modulus	Normal(1.001103E_n,0.01)	[43]
* s_c=standard deviation for characteristic strength (in MPa) of concrete as given in IS 1343[34]			

Table 2: Deterministic Parameters

Parameter	Description	Values taken
p	Percent reinforcement	0.2%
f_{ck}	Characteristic compressive strength of concrete	45 MPa
$f_{cn} = f_{ck}/1.5$	Nominal compressive strength of concrete	30 MPa
f_{yn}	Nominal yield strength of reinforcing steel	415 MPa
E_n	Nominal Young's modulus of reinforcing steel	200 GPa
e/*D*	Eccentricity of prestressing force	0
d/*D*	cover depth	0.05
void range	no concrete due to PS cables	0.5*D* to 0.6 *D*

Table 3: Distribution types of loads

Load type	Distribution type	C.O.V	Bias
Dead	Normal	0.1	1.0
Pre-Stress	Lognormal	0.15	1.2
Live (Ordinary)	Lognormal	0.15	1.0
Temperature	Gumbel	0.15	0.9
Accidental Pressure	Gumbel	0.15	0.8

S_i^n =nominal value of i^{th} strength/material parameter, γ_i^s = i^{th} strength/material factor, Q_i^n = the nominal value of the i^{th} load and γ_i^q = i^{th} load factor. Note that there is no separate resistance factor multiplying the nominal resistance (as in LRFD) since material partial safety factors have already been incorporated in computing the strength.

The nominal values generally are fixed by professional practice and thus are inflexible. Some of the *m* partial safety factors (often those associated with material properties) can also be fixed in advance. The remaining PSFs can be chosen by the code developer so as to locate the design point, and hence locate the limit state as alluded to above, and hence achieve a desired reliability for the structure. Such an exercise can be conveniently performed if the strength and load effect terms can be separated as above in which case the limit state equation can be normalized by the design equation:

$$\frac{M_{\text{cap}}}{M_{\text{cap}}^n} - \frac{M_{\text{app}}}{M_{\text{app}}^n} = 0 \tag{27}$$

The reliability problem now becomes:

Find $\gamma_1^s,...,\gamma_k^s,\gamma_1^q,...,\gamma_{m-k}^q$ such that

$$P\left[\frac{M_{\text{cap}}}{M_{\text{cap}}^n(\gamma_1^s,...,\gamma_k^s)} - \frac{M_{\text{app}}}{M_{\text{app}}^n(\gamma_1^q,...,\gamma_{m-k}^q)} \le 0\right] = \Phi(-\beta_T) \tag{28}$$

Table 4: Nominal load effects for the critical element in each group

Load case	Load effect					
	Nxx (ton/m)	Nyy(ton/m)	Nxy (ton/m)	Mxx (ton-m/m)	Myy (ton-m/m)	Mxy (ton-m/m)
	Group 1					
D	-9.61E+00	-1.22E+01	9.64E+00	-2.14E-01	-2.27E-01	3.91E-02
Ps	-4.44E+02	-4.77E+02	1.25E+02	1.53E+00	1.90E+00	-1.39E+00
Lo	-9.61E-01	-1.03E+00	2.82E-01	-3.37E-02	-3.63E-02	1.03E-02
T	3.12E+00	2.75E+00	1.34E+00	3.38E+00	3.42E+00	-1.27E-01
Pa	2.08E+02	2.26E+02	-7.09E+01	5.96E+00	6.29E+00	-1.30E+00
	Group 2					
D	-5.41E+01	-1.54E+01	2.80E+00	-8.11E+00	-1.31E+00	2.74E+00
Ps	-1.02E+03	-6.20E+02	-5.63E+01	3.55E+01	-5.00E+00	6.20E+00
Lo	-2.58E+00	-6.15E-01	3.18E-01	1.20E-02	1.27E-02	6.93E-02
T	1.56E+00	-1.28E-01	-4.86E-01	1.17E+01	2.78E+00	-1.90E+00
Pa	5.80E+02	1.50E+02	-7.01E+01	1.64E+01	-3.10E+00	-2.56E+01
	Group 3					
D	-2.65E+01	2.12E+00	6.12E+00	6.72E-01	-1.24E-01	-4.42E-02
Ps	-5.23E+02	-2.43E+02	2.42E+01	1.85E+01	8.95E+00	-2.07E+00
Lo	-1.04E+00	-3.24E-01	6.12E-02	-2.36E-02	-1.36E-02	-4.47E-04
T	-1.09E-01	5.88E+00	1.86E+00	4.56E+00	3.66E+00	-8.39E-02
Pa	2.46E+02	6.23E+01	-1.91E+01	-1.47E-01	1.98E+00	5.85E-01
	Group 4					
D	3.73E+00	-4.10E+01	2.24E-01	-1.34E-01	-6.23E-01	-1.18E-02
Ps	-6.70E+02	-5.32E+02	-1.89E+01	1.17E+00	-1.39E+01	-1.89E-01
Lo	2.55E-01	-8.37E-01	-2.62E-03	-4.52E-03	-2.28E-02	-4.45E-06
T	7.88E+00	5.93E-02	1.48E-02	5.01E+00	5.61E+00	-1.06E-02
Pa	2.85E+02	1.80E+02	1.77E+00	2.91E+00	1.23E+01	-8.57E-02

Table 5: Typical correlation matrix (group 1)

	Dead	Prestress	Live	Temperature	Pressure	M_{capxx}	M_{capyy}
Dead	1.0000	-0.0028	0.0005	0.0054	-0.0006	0.099	0.0117
Prestress	-0.0028	1.0000	-0.0028	-0.0093	0.0029	0.9156	0.9072
Live	0.0005	-0.0028	1.0000	0.0049	-0.0053	0.0036	0.0023
Temperature	0.0054	-0.0093	0.0049	1.0000	0.0060	-0.0176	-0.0156
Pressure	-0.0006	0.0029	-0.0053	0.0060	1.0000	-0.2935	-0.2972
M_{capxx}	0.0099	0.9156	0.0036	-0.0176	-0.2935	1.0000	0.9956
M_{capyy}	0.0117	0.9072	0.0023	-0.0156	-0.2972	0.9956	1.0000

Table 6: Bias and COVs of moment capacities

Group	M_{capxx}		M_{capyy}	
	Bias	COV	Bias	COV
1	1.82	0.159	1.41	0.157
2	1.65	0.133	1.42	0.171
3	1.40	0.137	1.59	0.149
4	1.58	0.133	1.54	0.145

Table 7: Optimization parameters

Parameter	Value
Target reliability, β_T	3.5
Tolerance on target reliability, $\Delta\beta$	1.0
Weights on four Groups, w_i	0.25, 0.25, 0.25, 0.25
Material PSF on concrete strength, γ_c	1.3
Material PSF on steel strength, γ_s	1.0
Lower bounds on load PSFs	1.0, 1.0, 1.0, 1.0, 1.3
Upper bounds on load PSFs	1.2, 1.2, 1.3, 1.4, 1.8

Table 8: Optimal results

Parameter	Optimal values
Beta values at optimum (Groups 1 – 4 respectively)	2.41, 3.88, 4.51, 4.25
Objective value (weighted squared error)	0.82
Optimal PSFs (D, P_s, L_o, T, P_a)	1.19, 1.09, 1.24, 1.35, 1.51

where β_T is the target reliability index. Of course, this is an under-defined problem and even though some of the PSFs may be fixed in advance as stated above, it has an infinite number of solutions. Additional considerations are needed to improve the problem definition. Such considerations naturally arise when PSFs are needed to be "optimized" for a class of structures and are discussed next.

It is common to expect that the design equation be valid for r representative structural components (or groups), and let w_i be the weight (i.e., relative importance or relative frequency) assigned to the i^{th} such component (or group). These r representative components may differ from each other on account of different locations, geometric dimensions, nominal loads, material grades etc. For a given set of PSFs, let the reliability of the i^{th} group be β_i. Choosing a new set of PSFs gives us a new design, a new design point, and consequently, a different reliability index. If there has to be one design equation, i.e., one set of PSFs, for all the r representative components, the deviations of all β_i's from β_T must in some sense be minimized. The design equation (Eq.(24) or Eq. (26)), when using the optimal PSFs obtained this way, can ensure a nearly uniform reliability for the range of components. Several constraints may be introduced to the optimization problem to satisfy engineering and policy considerations (as summarized in [42]). Moreover, some partial safety factors, such as those on material strengths, may be fixed in advance as stated above. The PSF optimization exercise adopted in this paper has the following form:

$$\min\left[\sum_{i=1}^{r} w_i \left(\beta_i\left(\gamma_1^q,...,\gamma_{m-k}^q\right)-\beta_T\right)^2\right] \text{ where } \sum_{i=1}^{r} w_i = 1$$
$$\text{subject to: } \min(\beta_i) > \beta_T, \quad i = 1,...,r \tag{29}$$
$$\gamma_i^q \geq \gamma_i^{\min}, \quad i = 1,...,m-k$$
$$\gamma_i^q \leq \gamma_i^{\max}, \quad i = 1,...,m-k$$
$$\gamma_i^s = m_i, i = 1,...,k$$

6. Numerical Example

An example problem based on the prestressed IC shells of typical 220 MWe Indian PHWRs has been set up to demonstrate the methodology developed in this paper. A combination involving 5 load cases namely Dead Load (D), Pre-Stressing Load (P_s), Ordinary Live Load (L_0), Accidental Temperature Load (T) and Accidental Pressure Load (P_a) has been considered. For each load case sets of six stress resultants (N_{xx}, N_{yy}, N_{xy}, M_{xx}, M_{yy}, M_{xy}) have been obtained from linear elastic finite element analyses. The FE model consisted of about 2500 elements.

Four structural groups of the IC Shell have been selected for finding optimal PSFs (Group 1: dome general area between two SG openings, Group 2: SG opening, Group 3: dome general area between SG opening and ring beam, Group 4: IC wall). The section depths (D) are respectively 500, 1200, 500 and 610 mm. For each group the critical element has been identified as the one having the lowest capacity demand ratio – by considering all nominal stress resultants for the given load combination. The objective of the example is to obtain a set of partial safety factors for the 5 applied loads that satisfy a set of optimality criteria.

The statistical parameters and nominal values used in the problem are listed in Tables 1 – 4. The computed correlation coefficients for Group 1 obtained between the moment capacities and applied moments are listed in Table 5. Noticeable here is the high positive correlation between moment capacity and prestressing force and the high negative correlation between the moment capacity and the accidental pressurization force. The moment capacities in x and y directions are almost fully mutually dependent. These are consistent with our intuitive expectations from the mechanics of the problem. The bias and COV of the moment capacities obtained for each group are

provided in Table 6. The optimization parameters (cf. Eq.) are listed in Table 7. While estimating the objective function in Eq. , a linear response was fitted around the given decision variable vector in order to smooth the sampling related fluctuations in the estimated reliability indices. Table 8 lists the optimal results for this example problem.

7. Conclusions

A set of optimal partial safety factors (for collapse limit state) ensuring a nearly uniform level of reliability across 4 groups of structural elements in a typical IC Shell of an Indian NPP have been obtained. The complete methodology for the same was developed from first principles. Correlations between demand and capacity terms owing to the structural mechanics underlying the problem were taken into account and the methodology developed accordingly. Analysis of the structural behavior of prestressed concrete section was formulated using recommendations provided in IS 1343 and SP 16. Monte Carlo simulations using (1) Importance Sampling and (2) a linear response surface fit for variance reduction was used to compute probabilities of failure. The load factors obtained in this example problem are in agreement with design practices from around the world, except the temperature load factor is typically lower than found here since thermal loads are categorized as secondary loads caused by geometric constraints and local yielding and micro-cracking ultimately result in redistribution of forces.

Acknowledgments

Support from BARC, Mumbai, India under the project titled "Development of reliability based criteria for containment design" is gratefully acknowledged.

References

1. Roy, R. and U. Verma, *Design issues related to containment structures of Indian PHWRs.* An International Journal of Nuclear Power, 2004. **18**(4): p. 44-57.
2. Ray, I., et al. *Evaluation of ultimate load bearing capacity of the primary containment of typical 540MWe Indian PHWR*. in *Smirt 17*. 2003. Prague.
3. CSE-3, *DESIGN OF NUCLEAR POWER PLANT CONTAINMENT STRUCTURE*. 2007, Atomic Energy Regulatory Board, Mumbai.
4. Shinozuka, M. and L.C. Shao, *Basic probabilistic considerations on safety of prestressed concrete pressure vessels.* Nuclear Engineering and Design, 1974. **29**: p. 338-345.
5. Ellingwood, B. and H. Hwang, *Probabilistic descriptions of resistance of safety-related structures in nuclear plants.* Nuclear Engineering and Design, 1985(88): p. 169-178.
6. Hwang, H., et al., *Probability-based load combinations for the design of concrete containments.* Nuclear Engineering and Design, 1985. **86**: p. 327-329.
7. Ellingwood, B., *Issues related to structural aging in probabilistic risk assessment of nuclear power plants.* Reliability Engineering and System Safety, 1998(62): p. 171-183.
8. Pandey, M.D., *Reliability-based assessment of integrity of bonded prestressed concrete containment structures.* Nuclear Engineering and Design, 1997(176).
9. Bhattacharya, B., R. Basu, and K.-t. Ma, *Developing target reliability for novel structures: the case of the Mobile Offshore Base.* Marine Structures, 2001. **14**(12): p. 37-58.
10. ISO, *ISO 2394 General Principles on Reliability for Structures*. 2 ed. 1998: International Organization for Standardization.
11. JCSS, *Probabilistic Model Code, 12th Draft*. 2001, Joint Committee on Structural Safety.
12. Wen, Y.-K., *Minimum lifecycle cost design under multiple hazards.* Reliability Engineering and System Safety, 2001. **73**: p. 223-231.
13. DNV, *Structural Reliability Analysis of Marine Structures*. 1992: Det Norske Veritas, Norway.
14. Galambos, T.V., *Design Codes*, in *Engineering Safety*, D. Blockley, Editor. 1992. p. 47-69.
15. Wen, Y.K., Collins, K.R., Han, S.W., Elwood, K.J., *Dual-level designs of buildings under seismic loads.* Structural Safety, 1996. **18**(2/3): p. 195-224.
16. CSA, *General Requirements, Design Criteria, the Environment, and Loads. A National Standard of Canada*. 1992, Canadian Standards Association.
17. ABS, *Draft Mobile Offshore Base Classification Guide*. 1999, American Bureau of Shipping, Houston, TX.
18. Ghosn, M. and F. Moses, *Redundancy in highway bridge superstructures*. 1998, Transportation Research Board: Washington, DC.
19. Nowak, A.S., M.M. Szerszen, and C.H. Park. *Target safety levels for bridges*. in *7th International Conference on Structural Safety and Reliability*. 1997. Kyoto, Japan.
20. E.D.F, *Design and Construction Rules for Civil Works of PWR Nuclear Islands, RCC-G, Volume 1-Design*. 1988, Electricite De France, Paris, France.
21. USNRC, *Seismic and Geologic Siting Criteria for Nuclear Power Plants, 10 CFR Part 100, Appendix A*. 1973, Recently revised on Jan 10,1997,US Nuclear Reculatory Commission.
22. Cave, L. and W.E. Kastenberg, *On the application of probabilistic risk assessment to reactors with inherently safe features.* Nuclear Engineering and Design, 1991(128): p. 339-347.
23. SEAOC, *Visiion 2000, Performance based seismic engineering of buildings*. 1995, Structural Engineers Association of California.
24. ATC-40, *Siesmic evaluation and retrofit of existing concrete buildings*. 1996, Applied Technology Council, Redwood City (CA).
25. FEMA, *FEMA 273, NEHRP guidelines for the siesmic rehabilitation of buildings; FEMA 274, Commentary*. 1996, Federal Emergency Management Agency.
26. Kinali, K. and B.R. Ellingwood. *Performance of non-seismically designed PR frames under earthquake loading*. in *Int. Conf. on Applications of Statistics and Probability (ICASP 10*. 2007. Tokyo, Japan.
27. Ghobarah, A., *Performance based design in earthquake engineering:state of development.* Engineering Structures, 2001. **23**: p. 878-884.
28. Raju, N.K., *Prestressed Concrete, 4th Edition*. 2007, New Delhi: Tata McGraw Hill.
29. A.S Al-Harthy, D.M.F., *Reliability assessement of prestressed*

concrete beams. Journal of Structural Engineering, 1994. **120**(1).

30. Hamann, R.A. and W.M. Bulleit. *Reliability of prestressed high-strength concrete beams in flexure*. in *Fifth International Conference on Application of Statistics and Probability in Soil and Structural Engineering*. 1987. Vancouver.
31. Varpasuo, P., *The seismic reliability of VVER-1000 NPP prestressed containment building.* Nuclear Engineering and Design, 1996. **160**: p. 387-398.
32. Wood, R.H., *The reinforcement of slabs in accordance with a predetermined field of moments.* Concrete (London), 1968. **2**: p. 69.
33. BIS, *IS 456:2000 Indian Standard Plain and Reinforced Concrete-Code of Practice (fourth revision)*. 2000, Bureau of Indian Standards, New Delhi.
34. BIS, *IS 1343 Code of Practice for Prestressed Concrete*. 2003, Bureau of Indian Standard, New Delhi.
35. Neville, A.M., *Properties of Concrete*. 4th ed. 1995, New Delhi: Pearson Education.
36. der Kiureghian, A. and P.-L. Liu, *Structural reliability under incomplete probability information.* Journal of Engineering Mechanics, ASCE, 1986. **112**(1): p. 85-104.
37. Ayyub, B.M. and R.H. McCuen, *Simulation-based reliability methods*, in *Probabilistic Structural Mechanics Handbook : Theory and Industrial Applications*, C. Sundararajan, Editor. 1995, Chapman Hall: New York.
38. Melchers, R.E., *Importance sampling in structural systems.* Structural Safety, 1989. **6**: p. 3-10.
39. Melchers, R.E., *Radial importance sampling for structural reliability.* Journal of Engineering Mechanics, ASCE, 1990. **116**(1): p. 189-.
40. Bjerager, P., *Probability integration by directional simulation.* Journal of Engineering Mechanics, ASCE, 1988. **114**(8): p. 1285.
41. Ellingwood, B.R., *LRFD: implementing structural reliability in professional practice.* Engineering Structures, 2000. **22**: p. 106-115.
42. Agrawal, G. and B. Bhattacharya, *Optimized partial safety factors for the reliability based design of rectangular prestressed concrete beams.* Journal of Structural Engineering, SERC Madras, 2010. **37**(4): p. 263-273.
43. Barakat, S., K. Bani-Hani, and M.Q. Taha, *Multi-objective reliability-based optimization of prestressed concrete beams.* Structural Safety, 2004. **26**: p. 311-342.

Appendix A: Wood's Criteria for Moment Combination

The design check is carried out in the principal plane with respect to stresses, which is inclined at an angle θ given by:

$$\tan 2\theta = \frac{2N_{xx}}{N_x - N_y}$$

On this plane shearing stresses are absent and the perpendicular (principal) stresses are given by:

$$N_1 = \frac{N_x + N_y}{2} + \sqrt{(\frac{N_x - N_y}{2})^2 + {N_{xy}}^2}$$

$$N_2 = \frac{N_x + N_y}{2} - \sqrt{(\frac{N_x - N_y}{2})^2 + {N_{xy}}^2}$$

The applied moments are converted to this plane according to standard tensor transformation procedures that lead to the following expressions:

$$M_{XX} = \frac{M_{xx} + M_{yy}}{2} + \frac{(M_{xx} - M_{yy})\cos 2\theta}{2} - M_{xy}\sin 2\theta$$

$$M_{YY} = \frac{M_{xx} + M_{yy}}{2} - \frac{(M_{xx} - M_{yy})\cos 2\theta}{2} - M_{xy}\sin 2\theta$$

$$M_{XY} = \frac{(M_{xx} - M_{yy})\sin 2\theta}{2} + M_{xy}\cos 2\theta$$

The moment capacity in direction1 and 2 (or X and Y) are then computed from interaction diagrams with transformed dimensions, reinforcement areas and voids. The applied moments in directions X and Y are obtained using Wood's Criteria. This outlines a procedure to obtain applied moments in X and Y direction at the bottom and the top of the section according to the following procedure:

Bottom Reinforcement

The bottom reinforcement can be calculated for following set of moments in x- and y- directions

$$M_x^* = M_{XX} + |M_{XY}|$$

$$M_y^* = M_{YY} + |M_{XY}|$$

If both M_x^* & M_y^* calculated as per the above equation are found to be negative, then both are assigned a zero value and not utilized for design. If M_x^* is negative, then

$$M_y^* = M_{YY} + \left|\frac{M_{XY}^2}{M_{XX}}\right| \text{and } M_x^* = 0$$

If M_y^* is negative, then

$$M_x^* = M_{XX} + \left|\frac{M_{XY}^2}{M_{YY}}\right| \text{and } M_y^* = 0$$

Top Reinforcement

The top reinforcement can be calculated for following set of moments in x- and y- directions

$$M_x^* = M_{XX} - |M_{XY}|$$

$$M_y^* = M_{YY} - |M_{XY}|$$

If both M_x^* & M_y^* calculated as per the above equation are found to be negative, then both are assigned a zero value and not utilized for design. If M_x^* is negative, then

$$M_y^* = M_{YY} - \left|\frac{M_{XY}^2}{M_{XX}}\right| \text{and } M_x^* = 0$$

If M_y^* is negative, then

$$M_x^* = M_{XX} - \left|\frac{M_{XY}^2}{M_{YY}}\right| \text{and } M_y^* = 0$$

The limit state in x direction (i.e, principal plane 1) and y directions are respectively:

$$M_{cap\_x} - \max(\text{abs}(M_{xtop}^*), \text{abs}(M_{xbottom}^*))$$

$$M_{cap\_y} - \max(\text{abs}(M_{ytop}^*), \text{abs}(M_{ybottom}^*))$$

Life Cycle Reliability and Safety Engineering
Vol.3 Issue 2 (2014) 15-24

Evaluation of Failure Probability of Expansion Bellow at RCB Containment Penetration of PFBR using Higher Order Response Surface Method

J. Mishra[1], P. Chellapandi[2], A. MeherPrasad[3], S. Narayanan[3]
[1]*Safety Research Institute, Kalpakkam, INDIA*
[2]*Indira Gandhi Centre for Atomic Research, Kalpakkam, INDIA*
[3]*Indian Institute of Technology Madras, Chennai, INDIA*
E-mail: jmishra@igcar.gov.in

ABSTRACT

Expansion bellows are an integral part of the pressure boundary in the nuclear power plants, when they are used in the Reactor Containment Building (RCB) penetrations as soft connection to mitigate the effects of differential movements between the penetrating pipe and containment shell. The expansion bellows at the RCB penetration of secondary sodium line of Prototype Fast Breeder Reactor experience high axial and lateral duty at normal operating condition. Since these expansion bellows has lower safety margin compared to other mechanical components as it operate in the plastic zone, they may provide a potential source of leakage of contaminations to atmosphere in the event of failure of their structural integrity. In this work evaluation of failure probability of expansion bellow using a computationally efficient method based on higher order response surface method is presented. The developed method use Chebyshev polynomial for estimation of order of stochastic variables in the Limit State (LS) function as well as for approximation of LS function. The developed method also facilitates the sensitivity analysis of LS without any additional computational cost.

Keywords*: Failure probability, Bellow, Response surface, Chebyshev polynomial, Fatigue*

1. Introduction

Expansion bellows are an integral part of the pressure boundary in the nuclear power plants. They are used in the containment penetrations as soft connection to mitigate the effects of differential movements between the penetrating pipe and containment shell [1]. Expansion bellows are also used as inline components in the pipeline or in the components like heat exchangers to provide flexibility for thermal expansion and to function as pressure containing elements. As piping penetration bellows, it is the last engineered barriers to prevent the release of radioactive materials to the atmosphere from containment. Therefore they are a potential source of leakage of contaminations to atmosphere in the event of failure of their structural integrity. This paper presents a methodology to estimate the probability of failure of expansion bellows at the Reactor Containment Building (RCB) penetration of secondary sodium line of Prototype Fast Breeder Reactor (PFBR).

American Society of Mechanical Engineers (ASME) Boiler & Pressure Vessel (B&PV) code, Section VIII, Div.-2 [2] has given the criteria for checking the stability and fatigue failure of the expansion bellows for the static or quasi-static load. These criteria need evaluation of equivalent axial duty from the axial, lateral and bending duty of the bellows, calculated from relative translational and rotational movement of ends of these bellows. Based on the equivalent axial duty, allowable numbers of cycles to prevent fatigue damage are determined from the equations given in reference-2. The allowable number of cycles have design margin of 3 on cycles and 1.25 on stress to account the effect of scatter of data, surface finish, atmosphere. The Expansion Joint Manufacturer Association (EJMA) standard also provides average fatigue life from best-fit curve [3]. However, the allowable number of cycle obtained from the EJMA is average number of cycle to failure without any design margin.

ASME B&PV, Section III, Div.-1, Subsection-NB for pipelines and components have design margin of 20 on cycles and 2.0 on stress on the best fit curve obtained from fatigue test on the specimen in the laboratory environment. The Section-III criteria document states

that these factors account for data scatter, size, surface finish and atmosphere etc. It appears that the margin on allowable number of cycles obtained from the EJMA standard and ASME Section-VIII, Div.-2 is lesser than that of safety related pipelines and components. This implies that failure probability of expansion bellow will be higher than other components and must be evaluated to demonstrate the achievement of target reliability of safety system containing expansion bellows.

One of the safety function performed by expansion bellow in the PFBR is for containment isolation at RCB penetration for secondary sodium pipelines. The secondary sodium line of PFBR, which is 500 MWe sodium cooled pool type fast reactor, is at the temperature of 525^0C and passes through RCB penetration between Intermediate Heat Exchanger (IHX) and surge tank. High temperature and large vertical length of the line cause large thermal expansion of this pipe segment. To accommodate this expansion four expansion bellows in series are provided at the RCB penetration. Isolation of RCB will be jeopardize if there will be any breach of structural integrity of these bellows. In view of safety importance of these expansion bellows, failure probability of these bellows is evaluated with a procedure based on response surface method. The brief details of procedure and evaluation of failure probability of expansion bellow at RCB penetration is explained in coming sections.

2. Procedure of Failure Probability Evaluation

If structural behavior of a component is defined by a function $g(\mathbf{X})$, where $g(\mathbf{X}) = 0$ being the Limit State (LS) function and $g(\mathbf{X}) \le 0$ being the failure domain, then failure probability based on reliability theory can be defined as [4,5]

$$P_f = P[g(\mathbf{X}) \le 0] = \int_{g(\mathbf{X})\le 0} f_{\mathbf{X}}(\mathbf{x}) d\mathbf{x} \quad (1)$$

where $f_{\mathbf{X}}(\mathbf{x})$ is the joint probability density function for the vector $\mathbf{X}$ of basic random variables comprising of loads, material strengths and dimensions. In general, the $f_{\mathbf{X}}(\mathbf{x})$ is rarely available and only marginal probability distribution function is used for analysis.

In structural reliability analysis, Monte Carlo Simulation (MCS) is a well-known technique to accurately estimate the failure probability, p_f, regardless of complexity of the system or the LS. But MCS becomes computationally intensive for structural reliability analysis of complex systems with low failure probabilities and MCS can be infeasible when the analysis requires a large number of computationally intensive simulations.

Considering the difficulties of the multi-fold integral of Eq.(1), methods like First Order Reliability Method (FORM) or Second Order Reliability Method (SORM) are also developed. These methods use either an analytical approximation of this integral or an analytical approximation of this integral in invariant form that are simpler to compute [6, 7, 8, and 9]. These methods require explicit or implicit LS functions defined a priori. In actual problems true LS cannot be easily expressed in analytical form.

In fact it is general practice in the NPP industry to use Finite Element (FE) analysis to study the behavior of complicated systems to realistically model loading, material, boundary conditions. Therefore, any reliability method for failure probability assessment of NPP components must be able to integrate the desirable features of FE analysis procedure. The method should also be computationally efficient to reduce computational efforts to an acceptable level.

2.1 Response Surface Method

The Response Surface Method (RSM) is a technique which can provide an efficient and reasonably accurate estimate of failure probabilities regardless of the complexity of the failure process of the actual system. It is used to approximate the original complex and implicit LS functions by simple and explicit LS functions. Thus, RSM avoid the disadvantages of Monte-Carlo simulation methods by replacing the true input–output relationship by an approximation function. Recent studies have shown that successive iteration of RSM by integrating with FORM gives reasonably good explicit approximation of LS function [10, 11]. These methods use a grid of experimental design points at which the response of actual LS is evaluated to determine the unknown coefficients of polynomial representing the response surface.

Unfortunately, the selection of experimental design points has no precise theoretical guidelines but has large influence on the estimate of failure property [12]. Also work carried out by Gavin et al. has shown that successive generation of response surface by integrating with FORM doesn't guaranty the convergence of failure probability [13]. The main reason for divergence of failure probability is due to improper selection of order of polynomial and region

of experimental design points. Gavin et al. suggested a method called HOSRSM, in which an algorithm to estimate the order of random variables using Chebyshev polynomial as basis function is proposed at the expense of some extra computation cost. Prior information about order of the random variables increases the robustness of RSM in approximating the LS.

Although, it is found that in many cases HOSRSM give reasonable approximation of the LS functions, yet there are cases where it gives erroneous results. Especially for the problem where order estimation of the variable is insufficient or the higher order terms are present as mix-term in LS. For example consider the simple equation with cosine terms as given in Eq.(2):

$$g(X) = X_2 + \cos(2X_1) + \frac{X_1}{5} + 3 = 0 \qquad (2)$$

The approximation of LS function using the algorithm proposed by Boucher et al [10] with second order polynomial is shown in the figure 1(a). It can be clearly seen that second order polynomial will not be able to align the true LS curve as it is of higher order. Figure 1(b) represents the approximation using the HOSRSM with of two different random number sets. This method fails to estimate the good approximation of LS because it incorrectly estimated the order of Chebyshev polynomial. As a further extension of the work carried by Gavin et al. on evaluation of failure probability using higher order RSM and remove some of its shortcoming a procedure called Higher Order Response Surface Method (HORSuM) is proposed for evaluation of failure probability. A brief description of this procedure and its application for the evaluation of failure probability of expansion bellow is next sections.

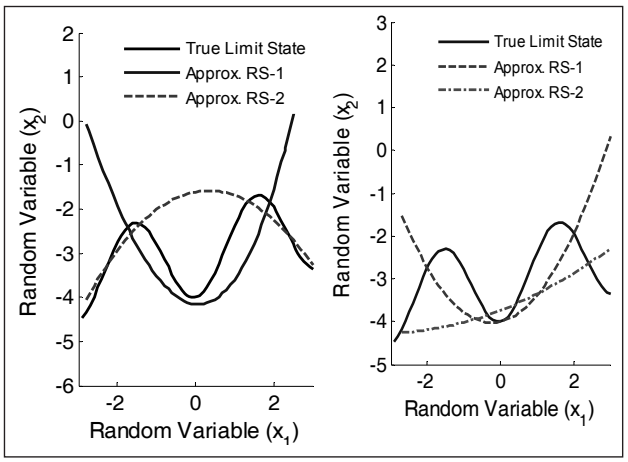

Fig. 1: Approximation of True LS function using (a) iterative FORM (b) HOSRSM

2.2 Higher Order Response Surface Method (HORSuM)

The proposed method, HORSuM, approximates the true LS function using Chebyshev polynomial as basis function $T_m(x)$ instead of regular polynomial $R_m(x)$. The Chebyshev polynomial and regular polynomial of order *m* can be given by $T_m(x) = \cos(m\cos^{-1}(x))$ and $R_m(x) = x^m$ respectively. The approximate LS of arbitrary order with $T(x)$ as basis function can be given as Eq. (3) or in the expanded form as Eq. (4).

$$\hat{g}(\mathbf{X}) = a + \sum_{i=1}^{n}\sum_{j=1}^{k_i} b_{ij}T_j(X_i) + \sum_{q=1}^{m} c_q \prod_{i=1}^{n} T_{p_{iq}}(X_i)) \qquad (3)$$

$$\hat{g}(\mathbf{X}) = a + \sum_{i=1}^{n}\sum_{j=1}^{k_i} b_{ij}\cos(j\cos^{-1}(X_i)) + \sum_{q=1}^{m} c_q \prod_{i=1}^{n} \cos(p_{iq}\cos^{-1}(X_i)) \qquad (4)$$

where the coefficients b_{ij} correspond to uni-variate basis function, and the coefficients c_q correspond to multi-variate basis function. The polynomial order k_i, the total number of mixed terms *m*, and the order of a random variable in a mixed term p_{iq} are determined in the various stages of the proposed method. The Chebyshev polynomial is chosen for the basis function over regular polynomial because it satisfies the condition of discrete orthogonality, bounded between -1 to 1, and selection of Chebyshev nodes as experimental design points distribute the error in approximation of LS more uniformly in the sampled domain. The proposed algorithm has three steps for generation of approximate LS $\hat{g}(\mathbf{X})$: (a) identification of the orders k_i of the random variables in the $\hat{g}(\mathbf{X})$ (b) determination of number and types of mixed terms (c) estimation of the coefficients of $\hat{g}(\mathbf{X})$ and determination of probability of failure, P_f using $\hat{g}(\mathbf{X})$.

2.2.1 Polynomial orders

For a univariate function $\hat{g}_1(x)$ that interpolates function $g_1(x)$ at the *m+1* roots of $T_{m+1}(x)$, $\hat{g}_1(x)$ can be written as a combination of orthogonal Chebyshev polynomial function as given in Eq. (5):

$$\hat{g}_1(x) = \sum_{j=1}^{m}{}' d_j T_j(x) \qquad (5)$$

where prime indicates that the first term is to be halved (which is convenient for obtaining a simple formula for all the coefficient of d_j). The coefficient d_j is independent of each other therefore addition of

higher order Chebyshev polynomial doesn't affect the coefficient of lower order polynomial. Since actual LS function $g(\mathbf{x})$ is a multi-variate function, it is converted into uni-variate function $g_i(x_i)$ by sampling all random variables, except X_i, at $r_m = 0$. Whereas, random variables X_i is sampled at the $M+1$ roots of $T_{M+1}(x)$ given by

$$r_m = \cos(\pi\,(m-0.5)/(M+1)),$$

where $m = 1, 2, 3, \ldots\ldots\ldots, (M+1)$. (6)

The approximation of uni-variate $g_i(x_i)$ with highest order polynomial k_i is written as $\hat{g}_i(x_{im}) = \sum_{j=0}^{k_i}{}' d_j T_j(x_{im})$

where $m = 1, 2, 3, \ldots\ldots\ldots M$ such that $k_i \le M$ (7)

Using the discrete orthogonality relation from Eq.(6) we have,

$$\sum_{m=0}^{M} g_i(x_{im})T_i(x_{im}) = \sum_{j=0}^{k_i}{}' d_j \sum_{m=0}^{M} T_j(x_{im})T_i(x_{im}) = \sum_{j=0}^{k_i}{}' d_j K_j \delta_{ij} \tag{8}$$

where $K_0 = n+1$ and $K_j = (n+1)/2$ when $1 \le j \le n$. Thus coefficient of polynomial can be computed by means of formula

$$d_j = \frac{2}{n+1}\sum_{m=0}^{M} g_i(x_{im})T_j(x_{im}) \tag{9}$$

In fact, in many cases

$$\sum_{m=0}^{M} g(x_{im})T_i(x_{im}) = \sum_{j=0}^{n}{}' d_j \sum_{m=0}^{M} T_j(x_k)T_i(x_k) \tag{10}$$

are rapidly decreasing. Thus, the error in the approximation is dominated by numerically less significant higher order term. Also the error is oscillatory function distributed smoothly in the region of [-1, 1], which is a highly desirable property in the polynomial approximation. The algorithm takes seven Chebyshev nodes of $T_7(x)$ for order estimation upto the sixth order. Although more number of nodes can be taken but seven Chebyshev nodes gives sufficiently accurate estimate of coefficient of polynomial.

Instead of incremental testing of order from 3rd order to higher order as suggested by Gavin et al., the entire coefficients are estimated together. This eliminates the problem of odd and even function getting approximated with a very low order polynomial. It also helps in evaluating the order of those variables which appear in LS function in only higher order. Selection of order of random variables is carried with following criteria: (i) if coefficient is more than 0.01% of constant term than that order is considered significant , (ii) if coefficient is more than 1.0% of preceding lower order term than that order is also considered significant .

2.2.2 Mixed terms

In problems with many random variables, mix-terms (i.e. $T_{p_1}(x_1)T_{p_2}(x_2).....T_{p_n}(x_n)$, where p_1, p_2 and p_n are order of the polynomial $T(x_1)$, $T(x_2)$ and $T(x_3)$ respectively) increase rapidly with increasing order of polynomials. Thus a suitable procedure has to be developed to filter out the insignificant mixed terms towards contribution to LS approximation. The mixed order polynomials $T_{p_1}(x_1)T_{p_2}(x_1)$ are plotted in figure-2, where p_1 is equal to two and p_2 varies from one to four. The mixed order polynomials are not perpendicular to each other, but they are bounded between [-1, 1].

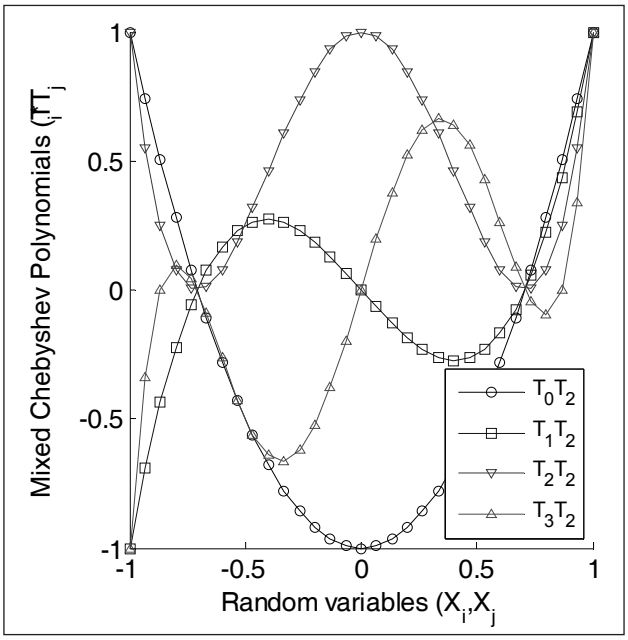

Fig. 2: Mixed Polynomial of order (T_iT_j)

The mixed order polynomials are not perpendicular to each other, but they are bounded between [-1, 1]. Also mixed order polynomials of even order, i.e. with their sum of $p_1, p_2, p_3, \ldots\ldots, p_n$ are even, fulfill the condition of discrete orthogonality with the mixed-order polynomial of odd order. The condition for this orthogonality is that the design points in the sample space must be mirror image about the origin. This property ensure that if a mixed order polynomial of even order is added in the approximate LS, it will have no influence on the coefficients of odd number mixed polynomial. Utilizing this property one can bi-furcated all the coefficients in odd and even order mixed

polynomial, and regression can be done separately. This reduces the number of LS iteration required for regression analysis for development of LS analysis.

To keep the number of deterministic evaluation of LS to minimum, stepwise forward selection procedure is employed for model building. The first step in the model building it is presumed to have all the term with their sum of order less than equal to minimum order, i.e. $\sum_i p_i \le \min(k_i)$. Subsequently, one term at a time is added in the model and following two criteria is employed to check the significance of added terms: (i) the polynomial coefficients corresponding to the added term are not less than 0.1% of maximum coefficients (ii) adding of the new terms improve the Adjusted R^2 of the regression model. Adjusted coefficient of determination R^2 is used for the checking the adequacy of the regression model in representing the relationship between regressor **X** and the response variables g(**X**). It represents the proportion of variability in response variable that is accounted for by the regression model and can be given by Eq. (11):

$$Adjusted\ R^2 = 1 - \frac{\left(\sum_{i=1}^{N}(\hat{g}(x_i) - g(x_i))^2\right)/(N - P)}{\left(\sum_{i=1}^{N}(g(x_i) - \bar{g})^2\right)/(N - 1)} \quad (11)$$

Where N is total number of sample points, p is total number of coefficients in the regression model and $\bar{g}$ is mean value of given by $g(x_i)$

2.2 3 Response Surface and Failure probability evaluation

Once all the terms involved for the estimation of response surface is identified, the coefficients are estimated using least squares method. Response surface is developed with Chebyshev polynomial as basis function instead of regular polynomial. It is worthwhile to mention here that polynomial order evaluation and mixed order evaluation are performed using Chebyshev polynomial; therefore further deterministic evaluation of LS function is not required. This significantly reduces the total number of deterministic analysis involved in the procedure. In the last stage, a full scale MCS on the approximated LS is carried out to determine the P_f.

The approximation of LS function using the HORSuM is shown in the figure-3. The accuracy and the efficiency of the HORSuM is compared with other methods like FORM, SORM, eHDMR and validation of the procedure is performed using full scale MCS. The validation work is not discussed in this paper. The failure probability of bellow using this method is explained in next section against LS based on fatigue failure.

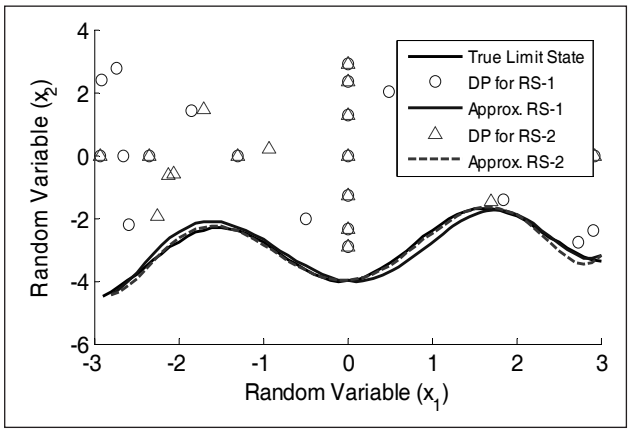

Fig.3: Limit state approximation using HORSuM

3. Finite Element Analysis of Expansion Bellow

3.1 Description of Bellow

Expansion bellows are part of the line segments which penetrated the RCB between IHX and surge tank. At normal operating conditions pipeline is at 525^{0}C, whereas in the shutdown condition it is at 150^{0}C. In case of draining of sodium from pipeline, it will reach the temperature of 40^{0}C. Expansion bellows will be approximately 50^{0}C lower than the pipeline temperature. Two expansion bellows are provided in both side of the containment wall to accommodate duty on the bellows at NOC. All these

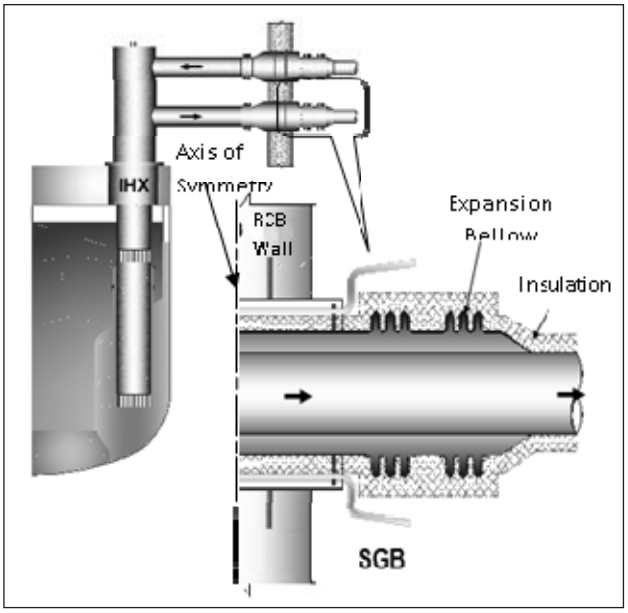

Fig. 4: Expansion bellows at RCB penetration in secondary sodium pipeline

bellows are attached with the sleeve in series. One end of this sleeve is welded with guard pipe inside RCB Containment and other end with the main pipe outside RCB containment. Middle portion of the sleeve is welded with the embedment penetration (EP) coming from the containment opening. Expansion bellows configuration near containment penetration is shown in the figure-4. The expansion bellow is made up of austenitic steel SS304L. The geometric details of these bellows are as given in Table-1 with their nomenclatures in figure-5.

Table 1: Geometric properties of the expansion joints

S.N	Geometric Properties	
1	Length of expansion joints (L)	: 440 mm
2	Inside Diameter of expansion joints convolution (Db)	: 840 mm
3	Convolution height (w)	: 29.5 mm
4	No. of corrugation(N)	: 10
5	Convolution pitch (q)	: 26 mm
6	End tangent length (Lt)	: 90 mm
7	Crest Convolution radius (ric)	: 7.5 mm
8	Root Convolution radius (rir)	: 7.5 mm
9	Design number of Cycles (N_{DBE})	: 1000

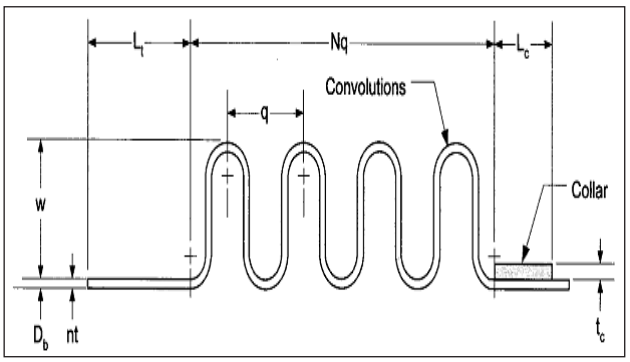

Fig.5: The sketch of the corrugation of expansion bellow

3.2 Finite Element Analysis

The FE element model is developed by meshing the area of solid model using 8-noded SHELL93 element. SHELL93 is particularly well suited to model curved shells. The element has six degrees of freedom at each node: translations in the nodal x, y, and z directions and rotations about the nodal x, y, and z-axes. The deformation shapes are quadratic in both in-plane directions [14]. An Integrated FE model of piping systems, which has pipeline modeled with pipe elements such as PIPE16 and PIPE18, and expansion bellows modeled with 8-noded shell element 'SHELL93', is developed for analysis. The connectivity between pipe and shell element is provided by a spider of beam element shown in figure-6. The material properties of bellows are taken RCC-MR [15] and ASME [2]. An elastic analysis of bellow is performed to evaluate the equivalent local membrane and bending stress for fatigue evaluation.

Fig.6: Finite element model of expansion bellow at the RCB penetration of PFBR

Pressure load on the expansion bellows is very low and the stresses induced due to pressure are insignificant. Only significant load at the normal operating condition is thermal expansion of pipe segment between IHX and surge tank. The Von Mises stress in the below at the inner surface is 708.34 MPa as shown in figure-7. The stress developed in the

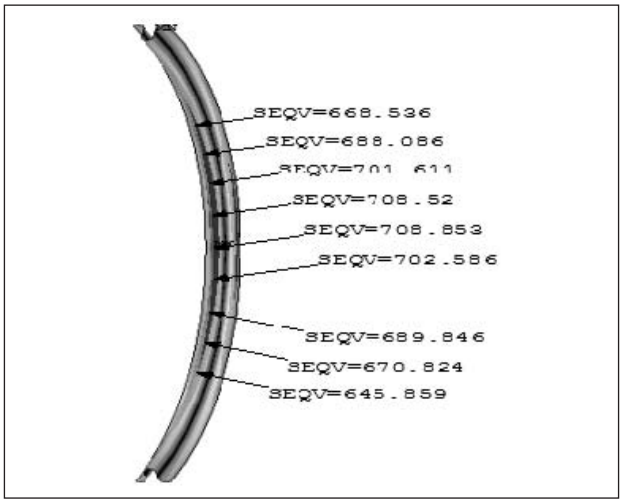

Fig. 7: Von Mises stress range in the expansior bellow curimg NOC

bellows is more than two times the yield strength of the bellow material and will not lead to shakedown of the bellow. Therefore fatigue-ratcheting due to thermal load became significant failure modes for bellow and considered as criteria of LS function formulation.

4.0 Failure Probability of Expansion Bellow

4.1 LS Function for Bellow

The secondary nature of thermal stress will lead to the gradual accumulation of plastic strain in the bellow and will cause failure of bellow due to low cycle fatigue. Therefore the LS for the bellow failure probability estimation is developed based on the fatigue failure criteria. Although several cumulative fatigue damage laws have been proposed, yet the Miner's hypothesis of linear cumulative damage is a good assumption, when cycles of small and large stresses are evenly distributed throughout the service life. In the present work Miner's hypothesis is used for the damage evaluation, where damage is simply the cycle ratio with basic assumptions of constant work absorption per cycle, and characteristic amount of work absorbed at failure [16]. The LS based on this assumption can be written as Eq.(12), Eq.(13) and Eq.(14).

$$g(X) = D_f - \frac{N_{DBE}}{N_{failure}} = D_f - \frac{N_{DBE}}{f(S_a, F_{curve})} \qquad (12)$$

$$S_a = f_1(t, OD, \Delta T, E) \qquad (13)$$

$$F_{curve} = f_2(F_{mds}, F_{se}, F_{sf}, F_{en}) \qquad (14)$$

Where, D_f is cumulative Damage ratio variable, N_{DBE} is number of full temperature cycles considered in the design basis events of PFBR, S_a is alternating stress intensity, *t* and *OD* are thickness and outer diameter of bellow respectively, ΔT is temperature range from shutdown to start-up, F_{mds} is factor for below material data scatter, F_{se} is the factor for size effect, F_{sf} is the factor for surface finish effect and F_{en} is the factor for environment effect. To reduce the number of variables a cumulative factor F_{curve} is selected to account for the effect of F_{mds}, F_{se}, F_{sf} and F_{en}. The uncertainties in these parameters are discussed in the next section.

4.2 Uncertainties in the Variables

The bellow is made up of material SA-240, Grade TP304L alloy steel. The minimum Young modulus (E) for this material at the temperature of 475^0 C specified in the RCC-MR is 157GPa. The Coefficient of Variation (COV) in young modulus is estimated as 0.031based on the 90% confidence bound given in the ref [17] for material 316LN. Assuming that minimum yield stress value is given at 95 percentile, mean of young modulus is estimated as 168.4 MPa.

The cumulative damage ratio variable D_f estimated from the Minor' hypothesis is load-sequence independent and lacks of load-interaction accountability. It can also be said that Minor's hypothesis does not distinguish between crack initiation and growth phases. It is observed that loads having the larger stress cycles near the beginning of life tend to accelerate failure which leads to $D_f \leq 1$. However, if the smaller stresses are applied first and progressively higher stresses follow, the cumulative damage ratio for failure $D_f \geq 1$. Therefore, D_f is taken as random variable with a mean value of 1 and COV of 0.1.

The best-fit fatigue curve for fatigue damage evaluation is generated from fatigue design curve given in the reference-2, which has a design margin of 3 of cycles and 1.25 on the stress. Also there is large dispersion in the data due to various factors like F_{mds}, F_{se}, F_{sf} and F_{en} affects the fatigue life. To account this dispersion a cumulative factor F_{curve} is developed to represent the uncertainties in these factors. The COV of the F_{curve}, estimated from the uncertainties in F_{mds}, F_{se}, F_{sf} and F_{en} reported in the literature [18, 19], is equal to 0.240. The best-fit fatigue curve (estimated mean fatigue curve) and design fatigue curve is shown in the figure-8.

The diameter of the bellow is 840 mm and its thickness is 0.63 mm. Diameter and thickness are

Table 2: Statistical properties of the random variables of expansion bellow

Random variables	Young Modulus (E) (GPa)	Fatigue Curve- F_C	Diameter- (OD) (mm)	Thickness (t) (mm)	Temperature Range (ΔT) (^{0}C)	Cumulative Damage Ratio (D_f)
Distribution	Lognormal	Weibull	Lognormal	Lognormal	Lognormal	Lognormal
Mean (μ)	168.4	As per Fig. 8	840	0.63	325	1.0
COV (Ω)	0.031	0.240	0.03	0.03	0.10	0.10

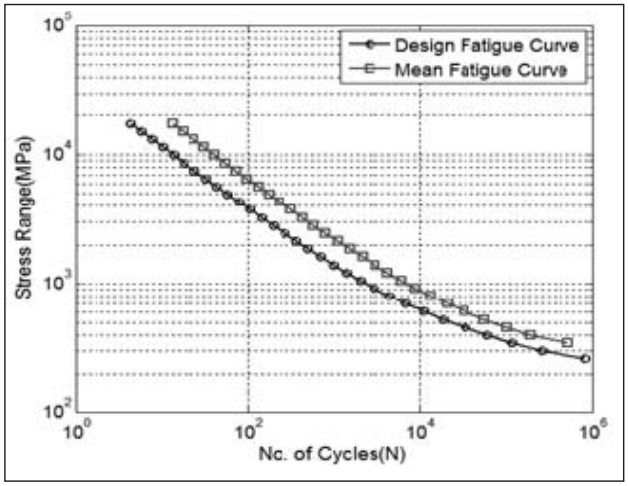

Fig.8: Fatigue Curve for bellow material SA-240, Grade TP304L alloy steel

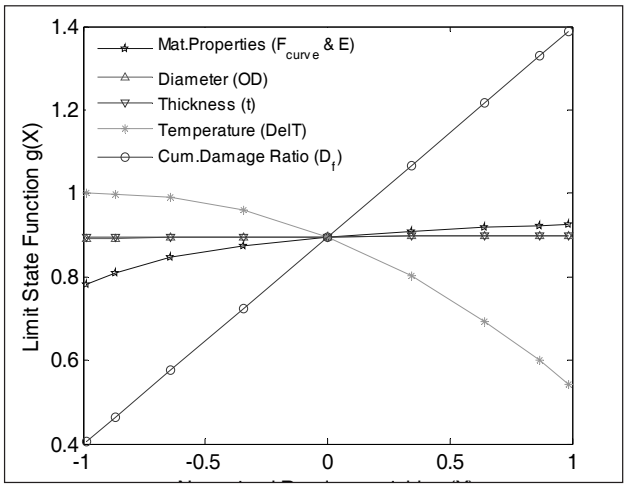

Fig. 9: Sensitivity of limit state function g(X) with random variables

considered as random variables with COV 0.03. The COV in temperature range is considered as 10%. Pressure load are very low on the bellow and treated as deterministic load in the analysis. Table-2 shows the statistical properties of the random variables of expansion bellow.

4.3 Order of Random Variables

The orders of random variables are determined as described in the section-2.2.1. A total of forty-one LS evaluations are performed for the estimation of the order of six random variables. The material properties of bellow defined by Young Modulus and fatigue curve are assumed to be correlated. This reduces the effective number of random variables to five. The order of random variables associated with material properties, diameter, thickness, temperature and cumulative damage ratio estimated by HORSuM is 6, 2, 2, 6 and 1 respectively. Figure-9 shows the graphical representation of sensitivity of LS function with random variables. It can be seen from this figure that there is strong dependence of LS with cumulative damage ratio, temperature and material properties, but relatively smaller dependence on thickness and outer diameter. The coefficients of polynomial of various orders shown in the Table-3 represent the numerical significance of that polynomial in the LS function simulation.

4.4 Coefficient Estimation of LS Function

Once the polynomial order gets estimated, next step is estimation of significant mixed order terms from hundreds of mix-terms. This is carried out as explained in the procedure HORSuM. The most significant ten terms of approximate LS function is shown in the Table-4. The polynomial order has five digits, where each digit symbolizing the order of random variables. The sequence of digits for the polynomial order is material properties, diameter, thickness, temperature and cumulative damage ratio respectively.

4.5 Failure probability of Expansion Bellow

The failure probability of expansion bellow is estimated with FORM using the approximated LS function developed in the previous section. The failure

Table 3: Coefficient of polynomial order defining sensitivity of random variables w.r.t limit state function

S.N	Polynomial Order	Mat. Properties	Diameter	Thickness	Temperature	Cumulative Damage Ratio
1	T0	8.76E-01	8.95E-01	8.96E-01	8.32E-01	8.96E-01
2	T1	6.64E-02	2.53E-03	3.25E-03	2.31E-01	5.00E-01
3	T2	2.23E-02	1.12E-03	1.67E-04	6.45E-02	6.81E-05
4	T3	7.49E-03	7.70E-05	7.70E-05	2.31E-04	5.31E-17
5	T4	2.49E-03	3.69E-05	2.43E-06	1.73E-04	1.54E-05
6	T5	8.23E-04	3.75E-06	2.06E-05	2.65E-04	2.83E-05
7	T6	2.78E-04	2.82E-17	5.15E-18	2.67E-04	8.89E-05

Table-4: Significant coefficients of Chebyshev polynomial for limit state approximation

S.N	Polynomial Order	Polynomial Coefficients
1	00000	0.800
2	00001	0.503
3	00010	0.265
4	11211	0.161
5	10010	0.118
6	11011	0.118
7	10000	0.107
8	20211	0.104
9	12111	0.082
10	21111	0.082

probability obtained from this method is 6.304e-08. A more accurate result can be obtained from full Monte Carlo Simulation, but in this case it is not required as failure probability is very low. The number of LS evaluation i.e. number of deterministic FE analysis required for failure probability estimation is 108. This is the average value of five iterations carried out using five set of stochastic variables whose seed number are selected randomly and shown in Table-5

The nearness of the failure probability for various set of variables shows the robustness of the procedure. Also developed procedure is highly computationally efficient as Monte Carlo simulation will take minimum of 10^{10} number of simulation for same level of approximation of failure probability. The failure probability is of the order of 10^{-7}, which indicated that the expansion bellow will maintain the structural integrity with high reliability at the normal operating condition.

Table-5: Failure Probability of expansion bellow evaluated using HORSuM

S.N	Failure Probability (P_f)	Reliability Index(β)	No. of Iterations
1	5.071e-008	5.324	106
2	6.644e-08	5.275	116
3	6.071e-008	5.291	101
4	5.881e-008	5.297	115
5	7.851e-008	5.244	102
Average	**6.304e-08**	**5.286**	**108**

5. Conclusion

The expansion bellows of secondary sodium line at the RCB penetration are an integral part containment pressure boundary in PFBR. The deterministic analysis of bellow shows that they experience high axial and lateral duty at normal operating condition. The nature of loads shows that most probable failure mode is low cycle fatigue. The failure probability of these bellows is estimated using the method based on higher order response surface method. The proposed method, HORSuM, first accurately estimates the order of the Chebyshev polynomial required for LS approximation. Subsequently significant mixed order terms are selected based on their numerical significance and its contribution to adjusted R^2 of the regression model. Check for significant mixed order terms reduce the total number of terms in the approximating polynomial, thus save the unnecessary computation work. The procedure is integrated with a FEA code ANSYS for failure probability estimation.

Failure probability is estimated against low cycle fatigue failure criteria, which has strong dependence on cumulative damage ration, material properties and temperature range, but less significant dependence on geometric properties like thickness and diameter. Probability of failure of expansion bellow estimated by HORSuM, which required only108 number of deterministic evaluation, is 6.304e-8. The failure probability is of the order of 10^{-8}, which indicated that the expansion bellow will maintain the structural integrity with high reliability at the normal operating condition.

References

1. Lambert L. D., and Parks M. B. , "Experimental results from containment piping bellows subjected to severe accident conditions", NUREG/CR-6154, SAND94-1711, Vol 2, 1994
2. "Rules for construction of pressure vessels-, ASME Boiler and Pressure Vessel Code, Section VIII, Division-2, Alternate Rules, American Society of Mechanical Engineers, 2010
3. "Standards of the Expansion Joint Manufacturers Association INC.". Ninth edition, 2010
4. Melchers, R.E., "Structural Reliability Analysis and Prediction", Ellis Horwood Limited., 1987.
5. Ditlevsen, O., and Madsen, H.O., "Structural Reliability Methods", John Wiley & Sons Ltd, Chichester, 1996.
6. Cornell, C. A., "A Probability-based Structural Code", ACI Journal, 66, 974-985, 1969.
7. Hasofer, A. M. and Lind, N.C., "Exact and Invariant Second Moment Code Format", J. Eng. Mech., ASCE Vol. 100 No. 1, pp. 111–121, 1974.
8. Chen, X., Lind, N.C., "Fast Probability Integration by Three-Parameter Normal Tail Approximation", Structural Safety vol. 1, pp. 269-276, 1983.
9. Ditlevsen, O., "Generalized second moment reliability index", J. Structural. Mechanics vol. 7, pp. 435-451, 1979.

10. Bucher C. G. and Bourgund U., "A Fast and Efficient Response Surface Approach for Structural Reliability Problems", Structural Safety, vol. **7**, pp. 57-66, 1990
11. Rajashekhar M. R. and Ellingwood B. R., "A New Look at the Response Surface Approach for Reliability Analysis", Structural Safety, vol. **12**, pp. 205-220, 1993.
12. Guan X.L. and Melchers R.E., "Effect of Response Surface Parameter Variation on Structural Reliability Estimates", Structural safety; vol. 23 pp. 429-444, 2001.
13. Gavin H. P. and Yau. S. C., "Higher-Order Limit State Functions in the Response Surface Method for the Structural Reliability Analysis", Structural Safety, Vol. 30 pp. 162-179, 2008.
14. ANSYS Inc. Manual, 2004
15. Design and Construction Rules for Mechanical Components of Nuclear Installations, RCC-MR, Section 1- Subsection Z, Appendix A3: Characteristics of Materials, 2007
16. Fatemi, A. and Yang L., "Cumulative Fatigue Damage and Life Prediction Theories: A Survey of the State of the art Homogenous Materials",Int. J. Fatigue Vol. 20 No. 1 pp.9-34, 1998
17. Riou B, M., Perandio S. and Guinovart J., "Material Variability in Elastic Assessment", Proceedings of a Technical Committee Meeting on Creep-Fatigue Damage Rules for Advanced Fast Reactor Design, Manchester, United Kingdom, 1996
18. Chopra O. K. and Shack W. J., "Review of the Margins for ASME Code Fatigue Design Curve - Effects of Surface Roughness and Material Variability", NUREG/CR-6815, ANL-02/39, 2003
19. Chopra O. K. and Shack W. J., "Effect of LWR Coolant Environments on the Fatigue Life of Reactor Materials", NUREG/CR-6909, ANL-06/08, 2007

Life Cycle Reliability and Safety Engineering
Vol.3 Issue 2 (2014) 25-31

Seismic Fragility Analysis of Structure, Systems and Components of Fast Breeder Test Reactor

C. Senthil Kumar[1], Ajai S. Pisharady[1], S. Usha[2], Prabir C. Basu[3]
[1]*Atomic Energy Regulatory Board, Mumbai, India*
[2]*Indira Gandhi Center for Atomic Research, Kalpakkam, India*
[3]*International Atomic Energy Agency, Vienna, Austria*
E-mail: cskumar@igcar.gov.in

Abstract

Seismic evaluation of a nuclear installation is a major safety concern. With the changing seismic design and safety requirements, it is also important to re-evaluate existing nuclear plants. In this context, a seismic re-evaluation exercise of a fast breeder test reactor (FBTR) at Kalpakkam is carried out. FBTR was built based on the design of Rapsodie-Fortissimo reactor and is in operation since 1985. Seismic Probabilistic Safety Assessment (SPSA)based on the IAEA guideline is undertaken to carry out the seismic re-evaluation of FBTR. The safety objectives for re-evaluation are identified as (i) safe shutdown of the plant (ii) maintaining in safe shutdown condition, (iii) long term decay heat removal, and (iv) containment of radioactivity. The major steps involved in SPSA are the probabilistic seismic hazard analysis (PSHA) to determine seismic demand in probabilistic format; safety analysis based on event tree - fault tree approach to identify the structures, systems and components (SSC) to be re-evaluated; determination of system capacity in terms of, seismic fragility from that of components; finally plant fragility culminating to risk quantification. Fragility analysis of SSC is an important activity for Seismic PSA.To apply the SPSA methodology to Indian scenario, number of innovative approaches is worked out, especially in the area of fragility analysis. The fragility of components is derived adopting analysis, testing and experience based method for their qualification. The present paper will describe the different approaches adopted in the seismic fragility analysis of the components and systems of FBTR. The methodology is discussed with the example of fragility analysis of a decay heat removal system viz., Preheating and emergency cooling system of FBTR.

Keywords: Seismic PSA, safe shutdown, fragility analysis.

1. Introduction

Seismic fragility of an item of structures or equipment or a safety system, is defined as the conditional probability of its failure for a given value of the input parameter such as stress, moment, spectral acceleration, peak ground acceleration (PGA). The objective of fragility evaluation is to estimate the PGA value for which the seismic response of a given component (i.e. structural elements or equipment) located at a specified point in the structure exceeds the component capacity resulting in its failure. Estimation of this ground acceleration value, called the ground acceleration capacity of the component, is accomplished using information on plant design bases, responses calculated at the design and analysis stage, and as-built dimensions and material properties. Because there are many sources of variability in the estimation of this ground acceleration capacity, the component fragility is described by means of a family of fragility curves. A probability value is assigned to each curve to reflect the uncertainty in the fragility estimation, usually in terms of non-exceedance probability. The component fragilities form the input in the system model to obtain Seismic Core Damage Frequency (SCDF) or seismic margin of the plant. This paper deals with the new approaches adopted for seismic fragility analysis of SSC in estimation of SCDFof FBTR.

The FBTR is a 40 MWt, loop type, sodium cooled fast reactor, operating at IGCAR, Kalpakkam since 1985. The reactor was built with French collaboration based on the design of the Rapsodie-Fortissimo reactor in Cadarache. Recently, a seismic re-evaluation of FBTR is carried out with the primary objective of reviewing the extent of seismic excitation FBTR can withstand without compromising its safety. In

order to achieve this, the seismic capacity of safety related structures, systems and components (SSC) of the plant required to achieve safety functions, viz., safe shutdown of the plant, maintaining the plant in safe shutdown, long-term decay heat removal and containment of radioactivity, are determined [1].

2. Plant Fragility of FBTR

Six potential initiating events are considered for evaluation of plant fragility of FBTR. Each of the initiating events is analysed using event tree approach to model the plant responses taking into account the associated frontline systemspresent to mitigate the progression of such unsafe events. The frontline systems are analyzed using fault tree approach to find all credible ways in which the undesired state (failure of the system) could be reached. (Fig. 1). To derive the seismic fragility of the plant, the Boolean expression for each accident sequence caused by an initiating event is derived and solved in terms of the fragility of SSC associated with the corresponding frontline system [2][3].

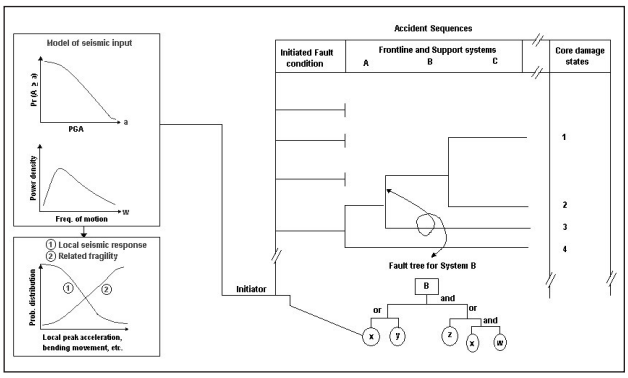

Fig. 1: Schematic of SPSA methodology

One of the initiating events viz.,Bothprimary WL drive system trip, considered for FBTR is shown in Fig. 2. Failure paths or the accident sequencesleading to unsafe states corresponding to this initiating event (IE1) are

Failure paths of IE_1= SQ3 or SQ6 or SQ9 or SQ10 or SQ13 or SQ14

Thus, probability of the plant reaching an unsafe state due to $IE_1$is evaluated as

$$P_f(IE_1) = 1 - \{(1 - P_f(\mathrm{SQ3})).(1 - P_f(\mathrm{SQ6})).(1 - P_f(\mathrm{SQ9})).(1 - P_f(\mathrm{SQ10})).(1 - P_f(\mathrm{SQ13})).(1 - P_f(\mathrm{SQ14}))\} \quad (1)$$

This way, the probability of seismic core damage of FBTR is evaluated from all initiating events as

$$P_f(\mathrm{Plant}) = \sum_{j=1}^{n} P_f(IE_j)$$

$$P_f(\mathrm{Plant}) = 1 - \{(1 - P_f(IE_1)).(1 - P_f(IE_2)).(1 - P_f(IE_3)).(1 - P_f(IE_4)) \dots \dots \dots (1 - P_f(IE_n))\} \quad (2)$$

where n is the total number of initiating events. Probability of occurrence of each accident sequence in (1) is determined from the Boolean expression of that path. E.g., the expression for the probability of occurrence of accident sequence 3, $P_f(SQ3)$ is

$$P_f(\mathrm{SQ3}) = P_f(IE_1).P_f(\mathrm{S5}).P_f(\mathrm{S6}) \quad (3)$$

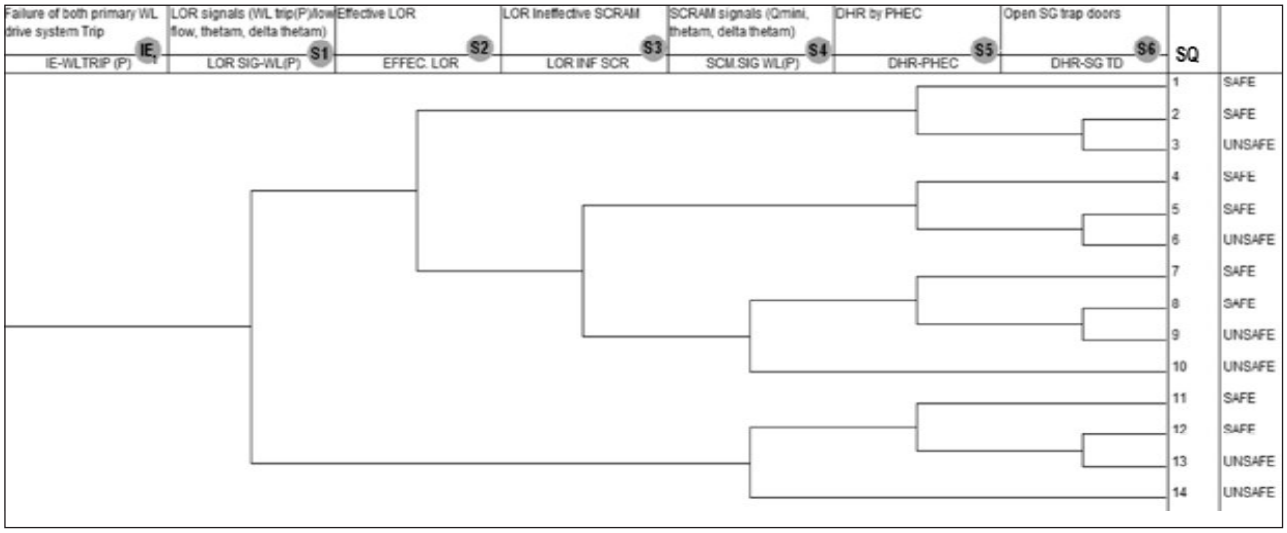

Fig.2: Event tree for failure of both primary WL drive system trip

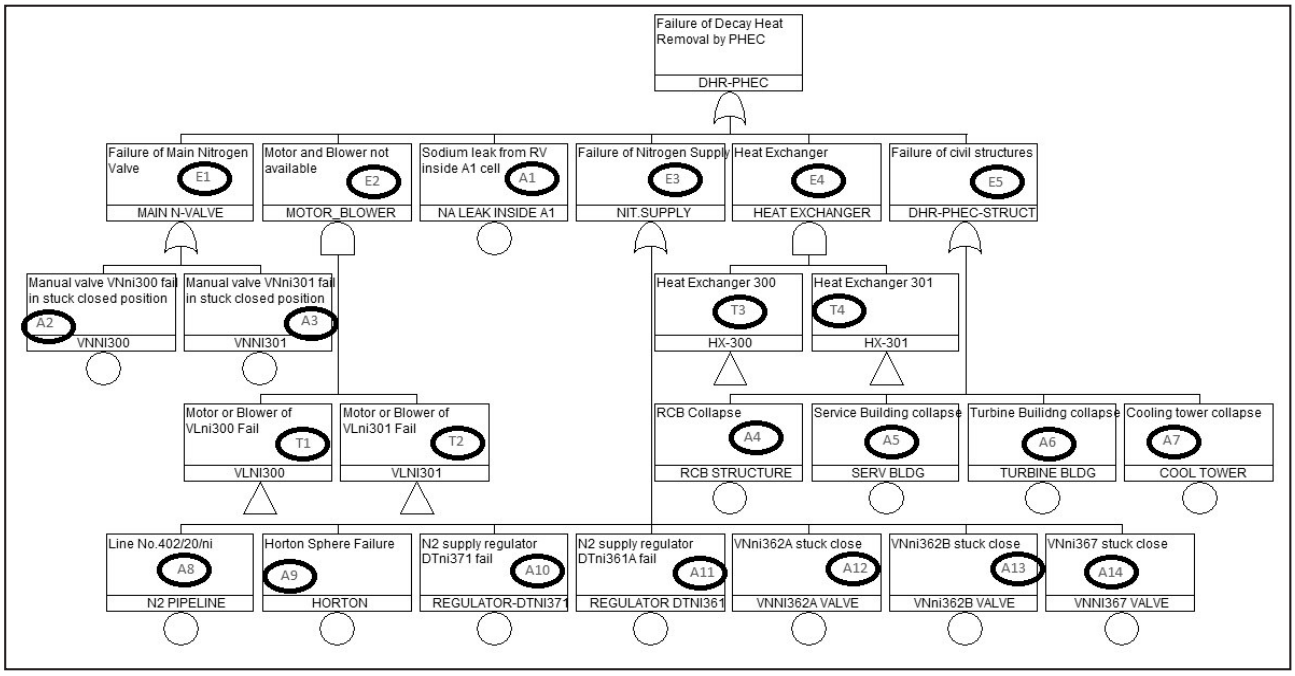

Fig.3: Fault tree for failure of Decay heat removal by PHEC

where, is the frequency of the initiating event 1; and are derived from the fault trees of system S5 and S6 respectively.

3. Determination of System Fragility

The fault tree corresponding to S5 viz., Preheating and Emergency Cooling system is given in Fig. 3. The Boolean expression for top event (PHEC system failure) of this fault tree derived from Fig. 3 is:

$$P(TE) = 1 - \{(1 - P_f(E1))(1 - P_f(E2)).(1 - P_f(A1)).(1 - P_f(E3)).(1 - P_f(E4)).(1 - P_f(E5))\} \quad (4)$$

Where:

$$P_f(E1) = 1 - \{(1 - P_f(A2)).(1 - P_f(A3))\}$$

$$P_f(E2) = P_f(T1).P_f(T2)$$

$$P_f(E3) = 1 - \{(1 - P_f(A8)).(1 - P_f(A9)).(1 - P_f(A10)).(1 - P_f(A11)).(1 - P_f(A12)).(1 - P_f(A13)).(1 - P_f(A14))\}$$

$$P_f(E4) = P_f(T3).P_f(T4) \text{ and } P_f(E5) = 1 - \{(1 - P_f(A4)).(1 - P_f(A5))(1 - P_f(A6)).(1 - P_f(A7))\};$$

T1, T2, T3 and T4 are transfer gates which are expanded further as separate fault trees and , etc, are the failure probability of basic component A1, A2, etc, respectively.

Failure probability of basic components is derived from the fragility description of the component that are available in terms of median ground acceleration capacity A_m and two associated random variables, ε_R and ε_U [6][7][8]. ε_R is a random variable representing the inherent randomness or epistemic uncertainties about the median value and ε_U is a random variable representing the aleatory uncertainty in the median value. ε_R and ε_U are log-normally distributed with have unit median and logarithmic standard deviations of β_R and β_U. The fragility i.e., the probability of failure P_f at any non-exceedance probability level Q can be expressed as:

$$P_f = \Phi\left(\frac{\ln\left(\frac{a}{A_m}\right) + \beta_U \Phi^{-1}(Q)}{\beta_R}\right) \quad (5)$$

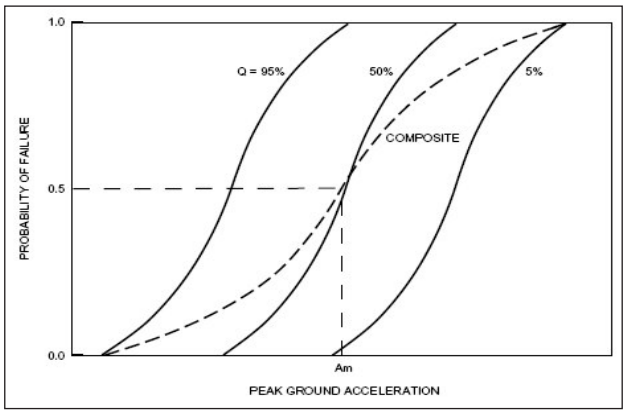

Fig.4: Typical family of fragility curves

where, $Q = P[P_f' < P_f|a]$ is the probability that the conditional frequency of failure, p_f', is less than p_f for a given peak ground acceleration, "a"; and Φ(.) is the standard Gaussian cumulative distribution function. From the (5), p_f is determined for discrete values of non-exceedance probability level such as 5%, 50% and 95% etc for each structural element, which then result in a family of fragility curves.Fig 4 depicts typical family of fragility curves of a component for various non-exceedance probabilities. The family of fragility curves is represented by the three components, viz. the median ground acceleration capacity, the logarithmic standard deviations representing epistemic randomness and aleatory uncertainty. The solid curve in the center represents, median fragility curve at 50% non-exceedance probability level. The logarithmic standard deviation of the randomness component determines the curve slope. The logarithmic standard deviation of the uncertainty component is a measure of the spread from the median curve. The 95thpercentile and 5th percentile curves in the figure are the upper and lower bounds of the probability of failure for a given acceleration, corresponding to 95% and 5% non-exceedance probability levels, respectively. The composite fragility curve is also known as the mean fragility curve and is shown as the dashed line in Fig. 4 for illustration. This curve represents the best estimate fragility description.

The composite fragility curve or the mean fragility curve is generated using the expression

$$P_f = \emptyset\left(\frac{1}{\beta_c}\ln\left(\frac{a}{A_m}\right)\right) \quad (6)$$

where $\beta_C = \sqrt{\beta_R^2 + \beta_U^2}$.

The HCLPF capacity of the component can also be determined from the fragility curve of that component. From the fragility curve, the PGA value corresponding to 95% confidence and having a probability of failure less than 5% is taken as the HCLPF capacity of the component.

Generally, the number of structures and components of concern may be very large and evaluation of fragility for all these components may not be feasible. Hence it is necessary to categorize the components and fragility would be addressed in terms of categories rather than components. For example, heat generators may form one category, safety related piping be another. The next three sections describe the procedures for determining the component fragility curves by direct as well as indirect methods.

4. Seismic Fragility of Component by Analytical Method

There are four major steps in deriving the seismic fragility of any component by analytical method:

- A component is considered to be an assemblage of elements. An element can have different failure modes. In the first step, the failure modes for elements of a component are identified.
- Fragility curve of an element for each of the identified failure modes are derived in the next step.
- The total element fragility curve is derived by combining element fragility curve for different failure modes.
- The component fragility curve is derived from the element fragility curves.

4.1 Failure modes of components:

Once the list of components for fragility evaluation is identified, the next step is to define the possible modes of failure for elements of the components. It is necessary to have a clear understanding of what constitutes failure of each element. Several modes of failure (each with a different consequence) may have to be considered and fragility curves may have to be developed for each of these modes. If an element has more than one dominant failure mode, the total element fragility is derived by combining the fragility derived for individual failure modes [10]. Probability of failure P_F of an element can be derived from its failure probability against a failure mode by adopting (i) series model, or (ii) parallel model, or (iii) combination of (i) and (ii). The first one is also known as the weakest link model, in which an element of SSC will not fail if it survives the seismic excitation against all possible failure modes. Therefore probability of survival, Ps, of the jth element is

$$P_{sj} = \prod_{i=1}^{n}\left(1 - p_{f_{ij}}\right),\ i = 1, 2, \ldots.n \quad (7)$$

Here, p_{fij} is the probability of failure of the jth element of a component against ith failure mode and n is the total number of failure modes. Therefore, overall probability of failure or failure probability of the jth element of a component for combined failure modes,

$$P_{Fj} = 1 - P_{sj} = 1 - \prod_{i=1}^{n}\left(1 - p_{f_{ij}}\right) \quad (8)$$

Eq.(8) assumesthat failure modes are independent. When failure modes are dependent, graded approach

can be adopted. An element will fail at i^{th} mode if it survives all the previous modes [11]. Therefore, failure probability of the j^{th} element in i^{th} mode is,

$$P_{f_{ij}} = \left[\prod_{k=1}^{i}\left(1 - p_{f_{kj}}\right)\right] p_{f_{ij}} \quad (9)$$

Probability of failure of the j^{th} element for combined mode

$$P_{f_{ij}} = 1 - \left(1 - p_{f_{1j}}\right)\prod_{i=2}^{n}\left(1 - \left\{\prod_{q=1}^{i-1}\left(1 - p_{f_{qj}}\right)\right\} p_{f_{ij}}\right) \quad (10)$$

4.2 Derivation of component fragility curve:

As mentioned earlier, a structure, system or component could be an assemblage of elements. When a component is an assemblage of elements, its behavior will depend on the performance of all, or a subset of, these elements. The fragility of such a component can be evaluated from the fragility of individual elements. These elements are connected together either in series or in parallel [12]. The elements are said to be in series, from fragility point of view, if only one element needs to fail for a failure of whole system. By contrast, a parallel system fails if all its elements fail. General structural configurations we encounter are not statically determinate systems, but are assumed as series systems. In series system, all the elements should survive to ensure system success. If probability of failure of element "*j*" is given by "P_j", and a structure, system or component has "*n*" such elements forming a series structural system, the probability of failure of thatparticular SSC can be represented as

$$P_F = \max_{j=1,2\ldots n}\left[P_{F_j}\right] \quad (11)$$

5. Seismic Fragility of Component by Testing

Fragility can be determined from qualification testing of components by adopting certain approximations. In seismic qualification testing, a component is subjected to input motion characterized by a specified waveform describing input level as a function of frequency. The component is qualified if it continues to perform its intended function when its response to this input motion (the test response spectrum, TRS) meets or exceeds pre-determined acceptance limits (the required response spectrum, RRS). However, qualification test data cannot directly be extrapolated to equipment capacity. Therefore, for equipment qualified by test, it is necessary to draw upon generic data to estimate the threshold of failure and use the test level to establish the tails of the fragility curves. In instances where equipment is tested to a high level, it can conservatively be assumed without compromising risk analysis results that the functional failure capacity is some modest level (about 25 percent) above the achieved test level with the test level defining the lower tail of the fragility curves [13]. The achieved test level is estimated to represent an acceleration level where there is 95% confidence that there is less than 5 percent probability of failure.

The estimation of median capacities from test results is almost always conservative, but in the absence of fragility data or analysis, it is the only reasonable method to establish fragility descriptions. Structural fragility of tested components will be estimated by using a factor of F_T over the test response spectra (TRS) for those cases where no distress is noted during or subsequent to the seismic qualification test. The factor, F_T includes the median factor which represents the ratio of test response to onset of distress, and the median of the ratio of response at the onset of distress to onset of failure. The value of F_T will range from 1.6 – 2.0 [15]. The median factor of safety, $\bar{F}$ is given by the product of F_T and lowest ratio of TRS to RRS over the frequency range of interest, i.e.,

$$\bar{F} = F_T . Lowest\left[\frac{TRS}{RRS}\right] \quad (12)$$

6. Seismic Fragility of Component by Walkdown

A walk down screening evaluation is an in-plant appraisal of the key physical attributes. Items that pass the screen are considered to possess adequate capacity. Items not passing the screen are of concern and detailed review or upgrade is necessary for these items depending on the potential risk. Seismic walk down is primarily based on the documented generic implementation procedure of Department of Energy (DOE-GIP) [16]. According to this procedure, there are four seismic screening guidelines used to evaluate the seismic adequacy of an item of equipment. They are:

- Seismic capacity compared to seismic demand
- Anchorage
- Seismic interaction
- Equipment class evaluation

Reference spectrum (RS) or generic equipment ruggedness spectrum (GERS) will be used to represent capacity while demand will be characterized by in-structure response spectrum. Components which satisfy the above four screening guidelines

are considered qualified for the considered RBGM level. Two approaches are identified for deriving the fragility curve for components [5]qualified by walk down viz., generic data approach and DOE-GIP based approach.

6.1 Generic data approach

Seismic fragilities are expressed in terms of a global parameter to the plant such as PGA of the design/review basis ground motion or related to the appropriate local response, rather than to the free-field seismic intensity [4][9][14][15][17][18][19].

6.2 DOE-GIP based approach

In this approach, component fragility curves are derived using (6).The median ground acceleration capacity Am is obtained fromthe median factor of safety $\bar{F}$ and the median value of RBGM-PGA, A_{RBGM} by the relation $A_m = A_{RBGM} \cdot \bar{F}$. The associated logarithmic standard deviations representing aleatory uncertainty, $\beta_U(.)$, and epistemic randomness $\beta_R(.)$ for different categories of components are provided by DOE-GIP. The median value of capacity factor F_C is given by the lowest ratio of RS/GERS to ISRS over the entire rangeof the spectrum,

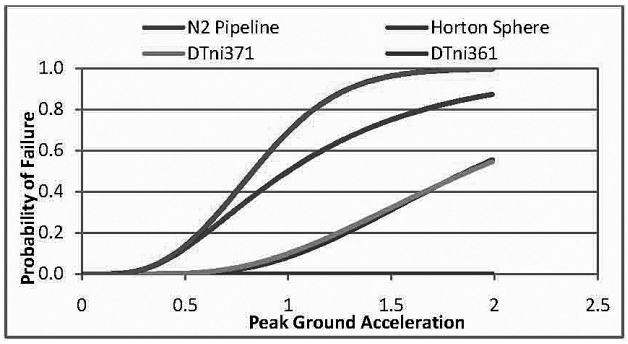

Fig.5: Fragility curves for Event E3 of PHEC system shown in Fig.3

$$\bar{F}_c = \text{Lowest}\left[\frac{\text{RS or GERS}}{\text{ISRS}}\right] \quad (13)$$

The generic values of equipment response factor $\bar{F}_{RE}$ and structure response factor for equipment are available in literature. Then, if {F(.)}'s follow log-normal distribution, the median $\bar{F}$ can be calculated from the median values {F(.)} as $\bar{F} = \bar{F}_c . \bar{F}_{RE} . \bar{F}_{RS}$.

7. PHEC System Fragility

For PHEC system, the list of components (SSC) obtained from Boolean expression given in (4), along with their qualification methodology, fragility

Table 1: List of SSC for PHEC

Component	Qualification Methodology	Am	βc	Prob. of failure
Horton sphere (A9)	Analysis	47.5	0.5	3.28E-27
Cooling Tower (A7)	Analysis	7.33	0.46	1.33E-14
RCB (A4)	Analysis	32.2	0.46	1.21E-27
Service Building (A5)	Analysis	1.13	0.46	2.02E-04
Manually operated nitrogen valves (A2, A3, A12, A13, A14)	Analysis	1.88	0.49	6.24E-06
PHEC heat exchanger (T3,T4)	Analysis	64.1	0.5	4.13E-30
Nitrogen Blowers VLni300,301 (in T1, T2)	DOEGIP	1.87	0.45	1.04E-06
Service Water header (in T3, T4)	Analysis	1.04	0.61	5.56E-3
Nitrogen Supply valve for Hx (in T3, T4)	DOEGIP	2.66	0.49	1.91E-07
Bus failure BTSB100A, 263B (in T1, T2)	DOEGIP	0.37	0.43	1.15E-01
Nitrogen Pipeline (A8)	Analysis	1	0.6	5.93E-03
Cable and cable penetrations (in T1, T2)	Testing	3.69	0.41	3.29E-12
Turbine Building (A6)	Analysis	1.75	0.46	3.37E-06
Service Water Pumps (in T3, T4)	DOEGIP	1.87	0.45	1.02E-06
Relay Latch contact (in T1, T2)	Testing	0.71	0.45	4.75E-03
Relays (in T1, T2)	Testing	1.8	0.45	1.57E-06
Manually operated valves-service water (in T3, T4)	Analysis	1.66	0.49	1.93E-05
Regulator (A10, A11)	DOEGIP	1.87	0.45	1.04E-06
Control and Limit Switches (AMrb14) (in T1, T2)	DOEGIP	0.71	0.45	4.75E-03

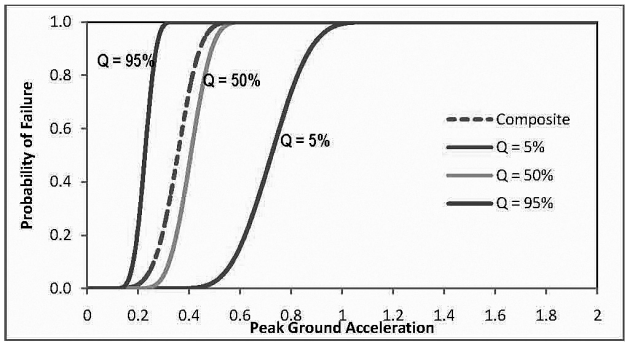

Fig.6: Fragility curves for PHEC system of FBTR

parameters and probability of failure is given in Table-1.

Using the fragility parameters (Table 1) in the Boolean expression, PHEC system failure probability is obtained. To illustrate the procedure, in Fig. 3, if we consider the event E3 that has seven components viz., Nitrogen pipeline, Horton sphere, regulators and manually operated nitrogen valves, probability of failure of all seven components are obtained from their respective fragility parameters using (6) and using the Boolean expression given in (4), probability of failure of the event E3 is obtained.

The composite fragility curve of the components and event E3 is shown in Fig. 5. Following the same procedure for other events in the fault tree, failure probability of PHEC system is obtained. At PGA value of FBTR system failure probability is 3.09E-2 and high confidence low probability of failure (HCLPF) of the system as 0.23g (Fig. 6). Plant fragility can be estimated by substituting the system failure probability in the accident sequences of initiating events.

8. Conclusion

Determination of component fragilities and the seismic margin capacity by probabilistic approach is explained. The methodology developed for deriving fragility curves for components is presented which can be appropriately used in the event trees to obtain plant fragility. The probabilistic approach adopted for estimation of plant fragility can be considered complementary to the deterministic approach. The paper also describes the procedure to obtain the Boolean expression of the accident sequences of event trees, frontline systems associated with the sequences and finally the list of SSC. The method is demonstrated with one of the decay heat removal system of Indian Fast Breeder Test Reactor.

References

1. Criteria and methodology for seismic re-evaluation of FBTR, Atomic Energy Regulatory Board and Indira Gandhi Centre for Atomic Research, India, AERB-IGCAR/ROMG/TN-658/01, November 2006.
2. INTERNATIONAL ATOMIC ENERGY AGENCY, Probabilistic Safety Assessment forSeismic Events, IAEA-TECDOC-724, Vienna (1993)
3. INTERNATIONAL ATOMIC ENERGY AGENCY, Seismic Evaluation of Existing Nuclear Power Plants, Safety Reports Series No. 28, IAEA, Vienna (2003).
4. INTERNATIONAL ATOMIC ENERGY AGENCY, Safety of new and existing research reactor facilities in relation to external events, Safety Reports Series No. 41, IAEA, Vienna (2005)
5. Report on Plant Walkdown, Atomic Energy Regulatory Board and Indira Gandhi Centre for Atomic Research, India, AERB-IGCAR/ROMG/TN-658/06-01, March 2008.
6. UNITED STATES NUCLEAR REGULATORY COMMISSION, PRA procedures guide, a guide to the performance of probabilistic risk assessments for NPP, NUREG CR-2300, Vol.2, USNRC, Washington.
7. Kennedy R P., etal, Probabilistic seismic safety study of an existing nuclear power plant. NED, 59 (1980), 315-338.
8. Kennedy R P., Ravindra M K., Seismic fragilities for nuclear power plant risk studies. Nuclear Engineering and Design, 79 (1984), 47-68.
9. Kennedy R. P, Etal., Subsystem fragility Seismic safety margins research Program (Phase I), NUREG CR-2405, Lawrence Livermore Laboratory, CA.
10. Basu P C. Ajai S. Pisharady, Seismic fragilities of reactor pressure vessel for combined failure modes, Proceedings of International conference on pressure vessel and piping, Chennai 2006.
11. Moses F., Kinser D E., Optimum structural design with failure probability constraints, AIAA journal, Vol. 6, No. 6 (1967), pp 1152 – 1158.
12. Casciati F. And FaravelliL., Fragility analysis of complex structural systems, Research studies press limited, Taunton, Somerset, England
13. Holman G.S., Chou C. K., Component fragility research program, Prioritization and demonstration testing, Lawrence Livermore National Laboratory, UCRL 95781, December 1986, LLNL, USA
14. J E. Wells Etal. NUREG CR - 4832: Analysis of the La Salle Unit 2 Nuclear Power Plant: Risk Methods Integration and Evaluation Program (RMIEP)
15. G. E. Bozoki, R. G. Fitzpatrick, M. P. Bohn, M. G. Sabek, M. K Ravindra, J. J. Johnson, 1994, NUREG/CR - 5726, Review of the Diablo Canyon Probabilistic Risk Assessment
16. DOE/EH-0545, Seismic Evaluation Procedure for US Department of Energy Facilities, U.S. Department of Energy, March 1977
17. UNITED STATES NUCLEAR REGULATORY COMMISSION, Seismic fragility of NPP components, NUREG CR-4659, Vol. 1-4, USNRC, Washington.
18. Park Y. J., Hofmayer C.H., Chokshi N. C., Survey of seismic fragilities used in PRA studies of nuclear power plants, Reliability engineering and system safety, 62 (1998), 185-195.
19. Cover L.E., Bohn M.P., Campbell R.D., Wesley D.A., Handbook of nuclear power plant seismic fragilities, (NUREG/CR-3558), USNRC, Washington.

Life Cycle Reliability and Safety Engineering
Vol.3 Issue 2 (2014) 32-37

Updating Reliability Models for existing Structures using Measured Responses

V. S. Sundar, C. S. Manohar
Department of Civil Engineering, Indian Institute of Science, Bangalore, India - 560012
E-mail: manohar@civil.iisc.ernet.in

Abstract

The problem of determining the posterior safety margin in randomly parametered and driven structures when data on measured responses become available is considered. The first step in the solution consists of system parameter and (or) force identification and this is followed by the solution of an inverse reliability problem posed as a constrained nonlinear optimization problem. The solution strategy consists of the application of Bayes' theorem, a modified version of subset simulations, and numerical optimization tools. The proposed method is exemplified by considering the analysis of an 11-member truss.

Keywords: Reliability model updating; FORM; MCMC; existing structures; inverse reliability analysis.

1. Introduction

Given a vector of random variables X with joint probability density function (jpdf) $p_X(x)$ and a performance function $g(X)$, the problem of reliability analysis consists of evaluation of the probability $P_F = \mathrm{P}\left[g(X) \le 0\right]$ [1,2]. For the case of existing structures, when measurement data set D becomes available, the problem of reliability model updating consists of evaluation of the conditional probability $P_{F|D} = \mathrm{P}\left[g(X) \le 0 \,|\, D\right]$ [3-8]. In the application of first and second order reliability methods (FORM and SORM), the random vector X is transformed into the standard normal space U with associated performance function $G(U)$ and one aims to obtain the reliability index $\beta_{HL} = \min_{G(u)\le 0} \sqrt{u^t u}$. Again, when the data D becomes available, one aims to find the posterior reliability index given by $\beta_{HL|D} = \min_{\beta_{HL}=\beta^*_{HL}} \sqrt{u^t u}$ with the fundamental problem here being the solution of the problem of system and (or) force identification encapsulated in the posterior jpdf-s $p_{X|D}(x|D)$ and equivalently, $p_{U|D}(u|D)$. In a recent paper [8] the present authors have outlined a procedure for the evaluation of $p_{U|D}(u|D)$ and $\beta_{HL|D}$. The approach here is based on application of Markov Chain Monte Carlo (MCMC) to sample from the posterior jpdf $p_{U|D}(u|D)$ characterized via the application of Bayes' theorem and subsequent development of an approximate model for $p_{U|D}(u|D)$ based on theory of Nataf's transformation [1]. An alternative approach to reliability consists of seeking to characterize the safety margin against a specified target reliability index, β^*_{HL}, and this class of problems is termed as inverse reliability problems. Here, instead of aiming to estimate P_F, one aims to find the available safety margin $M = \min_{\beta_{HL}=\beta^*_{HL}} G(u)$ [9-12]. In the present study we consider the problem of estimating the posterior safety margin $M_D = \min_{\beta_{HL|D}=\beta^*_{HL}} G(u|D)$ for existing structures when data D on measured responses become available. The solution strategy consists of the application of Bayes' theorem, a modified version of subset simulations, and numerical optimization tools. The proposed method is exemplified by considering the analysis of an 11-member truss.

2. Problem Statement

Consider the finite element (FE) model for a statically loaded structure with n degrees of freedom (dofs) governed by the equilibrium equation

$$K(X)Y + Q(X,Y) = P(X) \tag{1}$$

Here K is the $n \times n$ stiffness matrix, Q is a $n \times 1$ vector of functions which encapsulates the nonlinear structural behavior, P is the $n \times 1$ vector of nodal forces, and X is $p \times 1$ vector of system parameters which are modeled as a vector of random variables with prescribed jpdf $p_X(x)$. Let the structure be instrumented with s number of sensors yielding measurement data set $D = \left[Z_1 \quad Z_2 \quad \cdots \quad Z_N\right]$ where Z_k is the $s \times 1$ data vector resulting from the k-th episode of loading such that

$$Z_k = H_k(X, Y_k) + \nu_k \text{ with } K(X)Y_k + Q(X,Y_k) = P_k(X) \tag{2}$$

Here ν_k is a $s \times 1$ random vector which models the measurement noise and uncertainties in relating the measurement Z_k with the system state Y_k. In the present study we take ν_k to be Gaussian distributed with zero mean and covariance Σ_k. It is also assumed that ν_k and ν_j $\forall j \neq k$ are independent. Let β^*_{HL} be the specified target reliability index and the problem on hand consists of determining the posterior safety margin M_D after the data set D becomes available.

3. Solution Strategy

The solution to the problem of determining $M_D = \min_{\beta_{HL\mid D}=\beta^*_{HL}} G(u \mid D)$ is obtained using the following steps:

1. Determine the posterior pdf $p_{X|D}(x|D)$ by applying the Bayes theorem which yields [13]

$$p_X(x \mid D) = C\prod_{i=1}^{N} N\left[Z_i, H(x, Y_i), \Sigma_i\right] p_X(x) \qquad (3)$$

Here C is the normalization constant, $N[\bullet, \mu, \Sigma]$ is a multi-dimensional normal pdf with mean vector μ and covariance matrix Σ, and $p_X(x)$ is the apriori jpdf of X.

2. MCMC sampling: use algorithms such as Metropolis-Hastings or Gibbs sampler [14-15] and obtain N_s samples of X drawn from $p_{X|D}(x|D)$.
3. Construct a Nataf's model for X based on the N_s samples of X drawn from $p_{X|D}(x|D)$ and transform the performance function $g(X \mid D)$ to the equivalent function in the standard normal space denoted by $G(U \mid D)$.
4. Determine u^* which minimizes $M_D = G(u \mid D)$ subject to the constraint $\sqrt{u'u} = \beta^*_{HL}$. The optimal value of M_D is the updated safety margin being sought.

Details concerning implementation steps 1-3 have been discussed in our recent paper [8] and in the present work we focus on step 4.

4. Determination of Posterior Safety Margin

We employ three alternative schemes to determine $M_D = \min_{\beta_{HL\mid D}=\beta^*_{HL}} G(u \mid D)$. The first of these schemes is based on a modification to the subset simulation strategy used in the solution of forward reliability analysis problems [16] and other two schemes outline numerical optimization procedures to tackle the problem on hand.

4.1 Inverse Subset Simulation (ISS)

Here we develop a modification to the subset simulation (SS) procedure developed earlier in the work of [16,17]. The steps involved are summarized as follows:

1. Divide the target reliability index β^*_{HL} into l divisions $\beta^{(j)} = \beta^{(j-1)} + \Delta\beta;\ j = 2,3,\cdots l$ with $\beta^{(1)} = \Delta\beta = \beta^*_{HL}/l$. This leads to a set of l equally spaced concentric hyper-spheres in the standard normal space as shown in Fig. 1.
2. Set $k = 1$.
3. Simulate n_1 samples $\left(u_D^{(i)}\right)_{i=1}^{n_1}$ from $p_U(u \mid D)$.
4. Calculate for $u_D^{(i)}, i = 1,\ldots n_1$ the value of performance function, $G\left(u_D^{(i)} \mid D\right)$ and distance from the origin $\beta_D^{(i)} = \sqrt{\sum_{l=1}^{p} u_D^{(i)^2}}$.
5. Rank order the $u_D^{(i)}; i = 1, 2, \cdots, n_1$ according to ascending order of their corresponding $G\left(u_D^{(i)} \mid D\right)$.
6. From the rank ordered list, select the first n_0 points for which $\beta_D^{(i)} \geq \beta^{(k)}$. Denote this list by u_D^k, the corresponding distances by β_D^k and performance functions by G_D^k.
7. Define $g^k = \max\left[G_D^k\right];\ \beta_T^k = \max\left[\beta_D^k\right]$.
8. Starting from each of the n_0 samples, u_D^k, generate n samples from $p_{U|D}\left(u \mid G_D < g^k\right)$ using MCMC samplers.
9. Calculate for $u_D^{(i)}, i = 1, 2, \cdots n$ the value of performance function, $G_D\left(u_D^{(i)}\right)$ and the distance from the origin $\beta_D^{(i)} = \sqrt{\sum_{l=1}^{p} u_{l\mid D}^{(i)^2}}$.
10. Set $k = k + 1$.
11. Repeat steps 5 to 7.
12. If $\left|\beta_T^k - \beta^*_{HL}\right| \leq \varepsilon$, end the program; else go to step 8. Here ε is a user defined tolerance on satisfying the constraint $\beta_{HL\mid D} = \beta^*_{HL}$.
13. Denote by G^* the absolute minimum value of the safety margin obtained after the program terminates and by u^* the corresponding sample.

4.2 Gradient Projection Method (GPM) [18]

Here we form the Lagrangian $L = G(u \mid D) + \lambda\left(\sum_{i=1}^{p} u_i^2 - \beta^{*2}_{HL}\right)$ with λ being the Lagrangian multiplier and write the conditions for optimality a

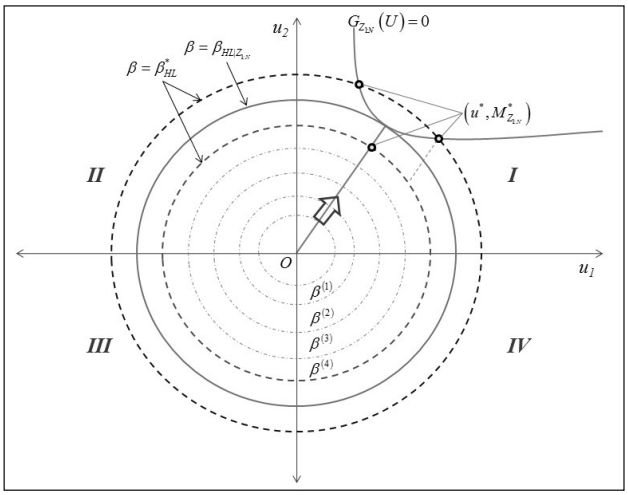

Fig. 1: Illustration of inverse subset simulation; dotted concentric circles denote the intermediate hyper-spheres; the arrow indicates the direction in which the simulated samples move.

$$\frac{\partial L}{\partial u_i} \equiv \frac{\partial G(u \mid D)}{\partial u_i} + 2\lambda u_i = 0,\ i = 1,2,\cdots,p$$
$$\frac{\partial L}{\partial \lambda} \equiv \left(\sum_{i=1}^{p} u_i^2 - \beta_{HL}^{*2} \right) = 0 \tag{4}$$

This set of $p+1$ nonlinear equations is solved using the Newton-Raphson method with an initial guess $u_i = 1,\ i = 1,2,\cdots,p$ and $\lambda = 1$ and convergence parameter $\varepsilon = 1 \times 10^{-6}$. It may be noted that when the performance function is implicitly defined the first order gradients and Hessian matrix need to be evaluated numerically.

4.3 Genetic Algorithm based Optimization (GAO) [19]

Here we use the *ga* toolbox available in MATLAB to solve the optimization problem on hand. Some of the algorithmic parameters used are as follows: initial population range: [-1, 1]; number of generations: 30; number of stall generations: 7; crossover fraction: 0.75; mutation fraction: 0.2; migration interval: 5; fitness level: 0.00001. This method does not require the evaluation of the gradients and hence is advantageous when the performance function is defined implicitly though a FE code. The algorithm leads to a global optimal solution and hence is expected to perform better than GPM and ISS methods.

5. Example

For the purpose of illustration we consider the pin jointed truss structure loaded as shown in Fig. 2. The structure is modeled using 14 dof FE method with linear axially deforming bar elements. The details of variables considered as being random are summarized in Tables 1 and 2, respectively. The performance function is defined with respect to initiation of yielding in member *GF*. The structure is taken to be instrumented by a set of five strain gauges, marked as $Z_1, Z_2, \cdots, Z_5$ in figure 2. The reliability analysis before assimilating measurements by using three methods, namely, FORM, brute force Monte Carlo simulations (MCS) and subset simulations (SS) is shown in Table 3. For the purpose of illustrations data on measurements are synthetically simulated

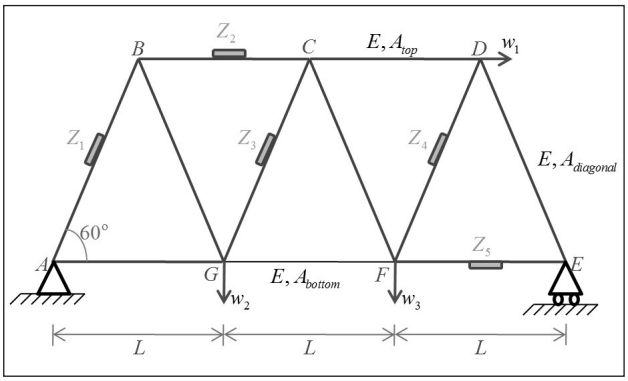

Fig. 2: Linear truss instrumented with 5 strain gauges $(Z_i)_{i=1}^{5}$

Table 1: Random variables and their distributions

Random Variable	Distribution (Mean, Standard deviation)
$X_1 = w_1$	Gumbel (49 kN, 4.9 kN)
$X_2 = w_2$	Normal (130 kN, 13 kN)
$X_3 = w_3$	Normal (130 kN, 13 kN)
$X_4 = f_y$	Lognormal (250 MPa, 17.5 MPa)
$X_5 = E$	Lognormal (210 GPa, 6.3 MPa)
$X_6 = A_{bottom}$	Lognormal (1000 mm^2, 30 mm^2)
$X_7 = A_{top}$	Lognormal (750 mm^2, 22.5 mm^2)
$X_8 = A_{diagonal}$	Lognormal (750 mm^2, 22.5 mm^2)
$X_9 = L$	Lognormal (3000 mm, 300 mm)

Table 2: Correlation between the random variables

Random variables	Correlation coefficient
X_1 and X_2	0.20
X_1 and X_3	0.10
X_7 and X_8	0.10
X_6 and X_7	0.15

Note: The other correlation coefficients are taken to be 0.

Table 3: Reliability analysis prior to the assimilation of measurements

Method	β_{HL}	P_F	u^*	x^*	$\partial\beta_{HL}/\partial u_i$	$\partial\beta_{HL}/\partial x_i$
FORM	3.7967	7.3327×10^{-5}	1.6091	4.8188×10^{4}	0.4238	0.0000
			-0.6628	1.4911×10^{5}	-0.1746	0.1157
			-2.8585	1.4976×10^{5}	-0.7529	-0.9919
			0.0000	2.0421×10^{8}	0.0000	0.0000
			0.6901	2.0991×10^{11}	0.1818	0.0000
			0.0000	9.6294×10^{-4}	0.0000	-0.0006
			0.7023	7.4548×10^{-4}	0.1850	0.0094
			-0.7953	7.4966×10^{-4}	-0.2095	-0.0062
			1.2701	2.9851	0.3345	0.0514
MCS (with 10^6 samples) followed by inverse analysis using GPM.	3.6350	13.9000×10^{-5}	1.5297	4.8180×10^{4}	0.4208	0.0000
			-0.6197	1.4814×10^{5}	-0.1705	0.1118
			-2.7611	1.4877×10^{5}	-0.7596	-0.9919
			0.0000	2.0561×10^{8}	0.0000	0.0000
			0.6452	2.0991×10^{11}	0.1775	0.0000
			0.0000	9.6528×10^{-4}	0.0000	-0.0007
			0.6671	7.4575×10^{-4}	0.1835	0.0108
			-0.7436	7.4966×10^{-4}	-0.2046	-0.0070
			1.2051	2.9851	0.3315	0.0588
SS	3.6649	4.7500×10^{-5}	-	-	-	-

Table 4: Measurements on strains

Members	1	2	3
AB	9.3327×10^{-4}	8.9710×10^{-4}	9.3153×10^{-4}
BC	9.8610×10^{-4}	9.2969×10^{-4}	9.2054×10^{-4}
GC	-9.0282×10^{-5}	-8.8672×10^{-5}	-8.5202×10^{-5}
FD	-1.1396×10^{-3}	1.2147×10^{-3}	-1.2280×10^{-3}
FE	-4.6646×10^{-4}	5.0874×10^{-4}	-4.2425×10^{-4}

using the FE model and seeded by noise; the details are as in Table 4. The measurement noise is taken to possess zero mean with standard deviation 4.6191×10^{-5}, 4.8915×10^{-5}, 4.4513×10^{-6}, 5.9554×10^{-5} and 2.2874×10^{-5} respectively for the five sensors. The moments of the system parameters following the identification step are shown in Table 5. Part of Table 6 shows the results on reliability model updating based on the identified system. The problem of assessing posterior safety margin is solved with target reliability of $\beta^*_{HL}=3.7967$ and the corresponding results from alternative solution schemes are summarized in Table 6. In absence of measurements this target reliability index corresponds to a safety margin of zero.

The time taken (on an Intel® Core ™ i5 650 @ 3.20 GHz with 8 GB of RAM) for the three methods to update safety margin, namely, ISS, GPM, GAO, are 16763.0s, 330.2s and 1617.2s, respectively. The following observations can be made from the numerical results obtained:

1. The effect of measurements made is observed to increase the structural reliability. This is evident from the results of forward reliability analysis (from which it is observed that apriori $\beta_{HL}=3.7967$ and posteriori index $\beta_{HL|D}=3.8798$) and from the assessment of safety margin from the inverse analysis (see from Table 6, first row, that $M_D>0$ as per all the three methods of analysis).
2. The differences in values of M_D as per ISS, GPM and GAO (2.6893, 1.7795, 1.2349 respectively; Table 6) are attributed to basic differences in the

method computational approaches. It is expected that the results based on genetic algorithm are superior to other results given the inherent ability of genetic algorithms to produce global optimal solutions.

3. If the updated safety margin is positive, it is expected that the three methods (namely, ISS, GPM, and GAO) would lead to similar results. On the other hand, if the margin is negative, ISS and GAO typically lead to multiple solutions while GPM could lead to unique solutions. Figure 3 illustrates this point. Here if, g_3 is the updated limit surface and β_3 is the target reliability, ISS and GAO are seen to lead to multiple solutions while GPM solution is unique.

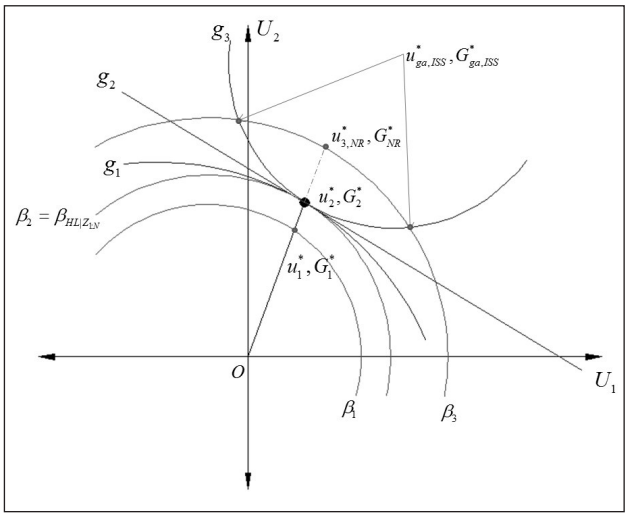

Fig. 3: Geometric representation for safety margin and point of minimum safety margin

Table 5: Results of system Identification

Parameter	Mean	Standard deviation
P_1	5.2592×10^4	4.3366×10^3
P_2	1.3744×10^5	4.5968×10^3
P_3	1.4742×10^5	4.6926×10^3
f_y	2.5336×10^8	1.6564×10^7
E	2.0621×10^{11}	5.5611×10^9
A_{bottom}	9.7780×10^{-4}	2.3746×10^{-5}
A_{top}	7.4503×10^{-4}	1.7966×10^{-5}
$A_{diagonal}$	7.5399×10^{-4}	1.4461×10^{-5}
L	2.9972	0.2546

6. Discussions and Conclusions

This paper considers the problem of determining the updated value of safety margin for existing instrumented structures when data on measured response of the structure become available. The solution strategy consists of a two-step procedure involving a system identification step followed by a reliability analysis step. The tools employed for the solution include application of Bayes' theorem, MCMC based sampling procedures, construction of non-Gaussian models for system parameters based on Nataf's transformation, and inverse reliability analysis based on a modified subset simulation scheme

Table 6: Results of updating of reliability and safety margin

FORM $\beta_{HL\|D} = 3.8798$, $P_{F\|D} = 5.2264 \times 10^{-5}$		Inverse analysis using **ISS** $(M_D = 2.6893)$		**Inverse analysis using GPM** $(M_D = 1.7795)$		**Inverse analysis using GAO** $(M_D = 1.2349)$	
u^*	x^*	u^*	x^*	u^*	x^*	u^*	0
0.3642	5.2504×10^4	0.5098	5.9360×10^4	0.3468	5.7374×10^4	0.3334	5.2725×10^4
-0.5032	1.4379×10^5	-0.7756	1.4424×10^5	-0.3879	1.4169×10^5	-0.7222	1.4286×10^5
-0.8995	1.5311×10^5	0.2919	1.5925×10^5	-0.7558	1.5462×10^5	-0.6984	1.5268×10^5
-0.6183	2.1221×10^8	-0.9980	2.1416×10^8	-0.4090	2.1292×10^8	-0.6555	2.1156×10^8
-1.0671	2.1393×10^{11}	-0.8626	2.1419×10^{11}	-1.0217	2.1363×10^{11}	-1.0466	2.1246×10^{11}
2.7780	9.3148×10^{-4}	2.3662	9.6930×10^{-4}	2.7092	9.4613×10^{-4}	2.7790	9.3663×10^{-4}
1.5800	7.4865×10^{-4}	1.8938	7.3822×10^{-4}	1.7183	7.4234×10^{-4}	1.6799	7.4284×10^{-4}
-1.4556	7.5775×10^{-4}	-1.0506	7.7419×10^{-4}	-1.0754	7.6330×10^{-4}	-1.1024	7.6011×10^{-4}
-0.0712	2.9490	-1.6448	2.8678	-0.9556	2.9470	-0.0967	2.9555

and numerical optimization methods. Numerical illustrations on an 11-member linear truss are provided based on synthetically simulated measurement data. Further work to extend the formulations to cover nonlinear structures, dynamic loads, and genuine experimental data is currently being carried out by the present authors.

Acknowledgement

This work is supported by a grant from the Board of Research in Nuclear Sciences, Department of Atomic Energy, Government of India and this is gratefully acknowledged.

References

1. Melchers R.E., "Structural Reliability Analysis and Prediction", Chichester, John Wiley & Sons, 1999.
2. Madsen H.O., Krenk S., and Lind N.C., "Methods of Structural Safety", Prentice-Hall, New Jersey, 1986.
3. Yao J.T.P., "Safety and Reliability of Existing Structures", Boston, Pitman, 1985.
4. Yao J.T.P., and Natke H.G., "Damage Detection and Reliability Evaluation of Existing Structures", Structural Safety, Vol 15, pp. 3-16, 1994.
5. Ellingwood B.R., "Reliability-Based Condition Assessment and LRFD for Existing Structures", Structural Safety, Vol 18, pp. 67-80, 1996.
6. Melchers R.E., "Assessment of Existing Structures-Approaches and Research Needs", Journal of the Structural Engineering, ASCE, Vol 127, No. 4, pp. 406-411, 2001.
7. Yao J.T.P., "Damage Assessment and Reliability Evaluation of Existing Structures", Engineering Structures, Vol 1, pp. 245-251, 1979.
8. Sundar V.S., and Manohar C.S., "First order and inverse reliability methods for updating reliability of existing structures using measured response".
9. Winterstein S.R., "Environmental Parameters for Extreme Response: Inverse FORM with Omission Factors", Structural Safety and Reliability, Vol 24, pp. 551-557, 1994.
10. Kiureghian A.D., "Inverse Reliability Problem", Journal of Engineering Mechanics. ASCE, Vol 120, pp. 1154-1159, 1994.
11. Foschi L.H., "An Inverse Reliability Method and its Application", Structural Safety, Vol 20, pp. 257-270, 1998.
12. Saha A., and Manohar C.S., "Inverse Reliability Based Structural Design for System Dependent Critical Earthquake Loads", Probabilistic Engineering Mechanics, Vol 20, pp. 19-31, 2005.
13. Beck J.L., and Au S.K., "Bayesian Updating of Structural Models and Reliability using Markov Chain Monte Carlo Simulation", Journal of Engineering Mechanics. ASCE, Vol 128, pp. 380-391, 2002.
14. Liu J.S., "Monte Carlo Strategies in Scientific Computing", Springer, New York, 2001.
15. Gilks W.R., and Richardson S., "Markov Chain Monte Carlo in Practice: Interdisciplinary Statistics", Chapman and Hall/CRC, 1996.
16. Au S.K., and Beck J.L., "Estimation of Small Failure Probabilities in High Dimensions by Subset Simulation", Probabilistic Engineering Mechanics, Vol 16, pp. 263-277, 2001.
17. Au S.K., and Beck J.L., "Subset Simulation and its Application to Seismic Risk Based on Dynamic Analysis", Journal of Engineering Mechanics, ASCE, Vol 129, pp. 901-917, 2003
18. Bertsekas D.P., "Constrained Optimization and Lagrange Multiplier Method", Athena Scientific, Belmont, Massachusetts, 1996.
19. Gen M., and Cheng R., "Genetic Algorithms & Engineering Design", first ed., Wiley-Interscience, New York, 1997.

Life Cycle Reliability and Safety Engineering
Vol.3 Issue 2 (2014) 38-44

Safety Assessment of Nuclear Power Plant Pipelines against Thermo-mechanical Fatigue in the Presence of Hybrid Uncertainties

M.B. Anoop, K. Balaji Rao
CSIR-Structural Engineering Research Centre, CSIR Campus, Taramani Chennai 600 113, INDIA
E-mail: anoop@serc.res.in

Abstract

Power plant piping components are subjected to a variety of thermal and thermo-mechanical loads, which include loads during hot shut down and cold shut down, in addition to the normal or steady operating loads of the power plant. A large number of piping failures in Pressurized Heavy Water reactors in the form of cracks and leaks due to these thermo-mechanical loads have been reported. Thermomechanical fatigue is one of the primary life-limiting factors for piping components in high temperature applications. In this paper, a procedure for the safety assessment of a nuclear power plant piping component against thermomechanical fatigue, by treating the relevant uncertain variables as random or fuzzy depending upon the source of uncertainty, is proposed. The fuzzy failure probabilities are computed using the method developed at CSIR-SERC, combining the vertex method with Monte Carlo simulation technique. The strain-based approach, which is the general approach employed for continuum response in safe-life, finite-life region i.e., the low cycle fatigue region with stabilized cyclic stress-strain constants, is used in the safety assessment. An example of a main steam piping of an operating thermal power plant is considered for illustrating the safety assessment procedure. It is also noted that one can determine the bounds for failure probability from the resulting fuzzy set for failure probability with minimal computational effort. The proposed procedure will help in rationally taking into account various uncertainties while designing the components with known/acceptable levels of safety specified either in codes or by learned bodies (AERB codes/NUREG).

Keywords: Thermomechanical fatigue; Power Plant Pipelines; Safety Assessment; Hybrid Uncertainties; Fuzzy Failure Probability

1. Introduction

Thermomechanical fatigue (TMF) is identified as a major degradation mechanism for engineering components such as nozzles, branch pipe connections, safe ends, welds, heat affected zone and base metal regions of high stress concentration, in many high-temperature applications. Nuclear power plant pipes are subjected to a variety of thermal and thermo-mechanical loads during their life cycle. These include loads during hot shut down and cold shut down, in addition to the normal or steady operating loads of the power plant. A large number of piping failures in Pressurized Heavy Water Reactors (PHWR) in the form of leaks and cracks due to these thermal loads have been reported (see Table 1).

A fundamental component of analysis of complex engineering facilities, such as nuclear power plants, is the appropriate incorporation and representation of uncertainty. The uncertainties in various factors such as variations in operating conditions inside the plant, material non-homogeneity, should be taken into account while assessing the safety of nuclear power plant pipelines against TMF. Probability theory has been traditionally used to represent both aleatory and epistemic of uncertainty. However, various researchers have pointed out that it may not be proper to use probability theory to represent the epistemic uncertainty in the presence of limited knowledge [1]. For instance, the safety assessment of nuclear power plant pipelines also involves information from expert judgment and/or data from in-service inspections. Fuzzy set theory will be more rational to represent the available data supplied by the experts. Hence, while the aleatory uncertainty can be modelled using the probability theory, it is more appropriate to represent the epistemic uncertainty using fuzzy set theory. In such circumstances, there is a need to develop special techniques, for carrying out the safety assessment, which can handle hybrid uncertainties (i.e. fuzzy and random).

Table 1 Some of failures due to thermal fatigue in PHWR [17]

Details of the plant	Location of failure	Reason for failure
Feedwater Piping		
Plant: Sequoyah Nuclear Power Plant, Units 1 and 2	Nozzles in Feedwater piping	Leaks, Crack growth induced by stresses from thermal stratification during cold, low-flow, feedwater injections.
Diablo Canyon Nuclear Plant Unit 1,1992	Nozzles of Feedwater piping lines to steam generators	Intermittent through-wall cracks upto 20 cm length in circumferential direction due to thermal fatigue. Cracks sized at 8.9 mm deep resulting from thermal fatigue leading to leaks
Donald C. Cook Plant, 1979	Feedwater lines to Steam Generators	Leaks
Reactor Coolant Systems		
Farley Nuclear Plant, Unit 2, 1987	Short unisolable section of a emergency core cooling system piping connected to the cold leg of a loop in RCS about 3 feet from the RCS cold leg nozzle	Leakage due to a circumferential crack (resulting from high-cycle thermal fatigue) extending through the wall in the heat affected zone of the weld between the first elbow and the horizontal pipe
Tihange	About 2 feet from the RCS hot leg nozzle.	Crack
Obrigheim	Weld between Nozzle to elbow closer to the RCS.	Crack
Dampierre, Unit 2	Weld between the check valve and straight pipe just upstream of the hot leg nozzle.	Crack
Dampierre, Unit 1	Base metal of the horizontal run between the hot leg and the check valve about 2 feet from the nozzle.	Leak
Biblis	Tee that connects a hot and a cold injection line	Crack
Genkai plant	Weld between the first elbow downstream of the hot leg nozzle and the horizontal run	Leak, Thermal stratification
Crystal River and Oconee 2	Centre of elbow extrados	Turbulent mixing of hot RCS fluid with cold makeup fluid behind the loose thermal sleeve
Westington plant	Tee between the Main pressurizer spray from the reactor coolant pumps and the cold auxiliary spray system.	Valve leakage, Thermal stratification
Loviisa Plant, Finland	Z-type isolation valve in an auxiliary spray line vertically above the main spray tee. Weld between reducer and tee that joins a hot leg and a cold leg drains	Leak Crack
Mihama	Excess let down line	Leak, crack located 15 inches from the reactor coolant loop inside the surface.
Three Mile Island	Cold leg drain line in the weld between the first elbow downstream of the loop nozzle and the horizontal run	Leak

Safety assessment of austenitic steel nuclear power plant pipelines against TMF in the presence of probabilistic and fuzzy uncertainties is presented in this paper. The relevant uncertain variables are treated as random or fuzzy depending upon the source of uncertainty. The fuzzy failure probabilities are computed using the procedure developed at CSIR-SERC, combining the vertex method with Monte Carlo simulation technique. The strain-based approach, which is the general approach employed for continuum response in safe-life, finite-life region i.e., the low cycle fatigue region with stabilized cyclic stress-strain constants, is used in the safety assessment for determining the thermo-mechanical fatigue life.

The paper is organized as follows. A brief description of TMF and the strain range partitioning model for TMF life prediction are presented in Section 2. The proposed approach for safety assessment of austenitic steel nuclear power plant pipelines against TMF in the presence of probabilistic and fuzzy uncertainties is presented in Section 3, followed by example in Section 4. The summary is given in section 5.

2. Thermo-mechanical Fatigue

TMF is a low-cycle fatigue occurring under simultaneous changes in temperature and mechanical strain. The major factors affecting the TMF life of a component are:

- Type of material
- Maximum and minimum temperatures: There is a substantial decrease in TMF life with increase in temperature or thermal loads [2].
- Strain ratio: TMF life decreases with increase in strain ratio (ratio of minimum strain to the maximum strain). However, in the plastic strain region the effects of strain ratio are considered negligible [3].
- Strain: Fatigue life decreases with increase in strain rate or strain range

The major difficulty in TMF life prediction is the interaction between fatigue and creep at varying temperatures. Numbers of models are proposed in literature for TMF life prediction [4]. Most of these models use damage-based criteria, stress-based criteria, strain-based criteria or energy-based criteria for TMF life prediction. The commonly used models for TMF life prediction are Damage Summation model, Frequency Separation model, Ductility Exhaustion model, Strain-Range Partitioning (SRP) model, Total Strain Version of SRP model, and Strain Energy Partitioning model. From a brief review of these models, it is noted that the modified strain range partitioning (SRP) method gives satisfactory predictions, especially for high temperature low-cycle fatigue. Hence, this method is chosen in the present study for predicting the TMF life of austenitic steel nuclear power plant pipelines. A brief description of the SRP model is given in the next section.

2.1 Strain-range partitioning model

The strain-range partitioning (SRP) model, proposed by Manson *et al.* [5] takes into account the time dependent portions of the fatigue cycle. In this model, the total inelastic strain-range is partitioned into time-independent plasticity and time-dependent creep. Each component contributes a certain fraction to the total damage. Thus, under cyclic reversed loading, there are four possible combination cycles of inelastic strain, namely, tensile plasticity reversed by compressive plasticity (PP), tensile creep reversed by compressive creep (CC), tensile creep reversed by compressive plasticity (CP), and tensile plasticity reversed by compressive creep (PC). In any stabilised combined cycle, a maximum of three cycle types are physically possible, PP, CC, and either PC or CP.

The SRP model [5] originally proposed was based on the following simple linear damage rule.

$$\frac{1}{N_f} = \frac{1}{N_{PP}} + \frac{1}{N_{CC}} + \frac{1}{N_{PC}} + \frac{1}{N_{CP}} \tag{1}$$

where N_f is the number of cycles to failure, N_{PP}, N_{CC}, N_{PC}, and N_{CP} are the fatigue lives produced by the PP, CC, PC and CP inelastic strain cycles, respectively. Use of SRP model requires four unique partitioned strain-ranges versus cyclic life relationships. These are obtained by carrying out four separate PP, PC, CC and CP creep-fatigue tests, and fitting the results of these tests to the Coffin- Manson Equation:

$$\Delta\varepsilon_{PP} = A_{PP}\left(N_{PP}\right)^{C_{PP}} \tag{2}$$

$$\Delta\varepsilon_{CC} = A_{CC}\left(N_{CC}\right)^{C_{CC}} \tag{3}$$

$$\Delta\varepsilon_{PC} = A_{PC}\left(N_{PC}\right)^{C_{PC}} \tag{4}$$

$$\Delta\varepsilon_{CP} = A_{CP}\left(N_{CP}\right)^{C_{CP}} \tag{5}$$

where $\Delta\varepsilon_{PP}$, $\Delta\varepsilon_{CC}$, $\Delta\varepsilon_{PC}$ and $\Delta\varepsilon_{CP}$ are the inelastic strain range components, the coefficients A and exponents C are experimentally determined material constants.

Based on the interaction damage rule, which uses strain-range fractions to partition damage, Manson and Halford [6] modified the SRP model. The modified SRP model can be expressed as [7]

$$\frac{1}{N_f} = \frac{F_{PP}}{N'_{PP}} + \frac{F_{CC}}{N'_{CC}} + \frac{F_{PC}}{N'_{PC}} + \frac{F_{CP}}{N'_{CP}} \quad (6)$$

F_{pp}, F_{cc}, F_{pc}, and F_{cp} are PP, CC, PC and CP strain-range fractions. For instance, $F_{pp} = \Delta\varepsilon_{PP}/\Delta\varepsilon_{in}$, where $\Delta\varepsilon_{in}$ is the total inelastic strain range. N'_{PP}, N'_{CC}, N'_{PC} and N'_{CP}, are the fatigue lives under PP, CC, PC and CP inelastic strain cycles, respectively. The values of N'_{PP}, N'_{CC}, N'_{PC} and N'_{CP} are calculated according to (2)-(5) using total inelastic strain range, $\Delta\varepsilon_{in}$, rather than the partitioned inelastic strain-range components (namely $\Delta\varepsilon_{PP}$, $\Delta\varepsilon_{CC}$, $\Delta\varepsilon_{PC}$ and $\Delta\varepsilon_{CP}$).

The procedure for determining TMF life is as follows:

1. Based on the cyclic stress versus strain response, obtain the partitioned inelastic strain-ranges, $\Delta\varepsilon_{PP}$, $\Delta\varepsilon_{CC}$, $\Delta\varepsilon_{PC}$ and $\Delta\varepsilon_{CP}$
2. Determine the strain fractions, F_{PP}, F_{CC}, F_{PC} and F_{CP}
3. Solve for N'_{PP}, N'_{CC}, N'_{PC} and N'_{CP} using (2)-(5) based on the total inelastic strain-range $\Delta\varepsilon_{in}$
4. Determine the TMF lives by the interaction damage rule using (6)

The TMF life determined using the above steps is for a theoretical zero mean stress condition. Halford and Nachtigall [8] modified the SRP model to incorporate the effect of mean stress. Some of the limitations of the SRP model [4] are:

1. The SRP model is not applicable to non-ductile materials. This is because, in general, the inelastic strains in these materials are very small so that it is difficult to determine correctly.
2. Since the SRP model does not consider the effect of oxidation, the TMF life may be over-predicted [9].
3. It is still difficult to partition the inelastic strain experimentally for TMF cycles. However, this can be overcome to an extent using the step-stress method proposed by Halford and Manson [10] and simplified step-stress method and the loop inversion method proposed by Nitta and Kuwabara [11].

3. Proposed Approach for Safety Assessment against TMF in the Presence of Hybrid Uncertainties

The variations in the operating conditions and the environmental conditions and variations in the micro-structural properties of the material of the piping component should be taken into account while assessing the safety of the piping component against TMF. This can be accomplished by treating the relevant variables as random or fuzzy depending upon the source of uncertainty. Different methods have been proposed by various researchers for handling fuzzy and random uncertainties together. In the present study, the approach proposed by Anoop *et al*. [12] that combines the vertex method with the Monte Carlo simulation (MCS) technique is used for determining the fatigue life. Vertex method, introduced by Dong and Shah [13], is a computationally efficient solution technique for computing functions of fuzzy variables. Suppose I_λ is the λ-cut interval, i.e., $I_\lambda = [a, b]$, of fuzzy set A. If fuzzy set B is image of A given by the mapping $B = f(A)$, then interval representing B at a particular value of λ, say B_λ, can be obtained by (7).

$$B\lambda = f(I\lambda) = [\min(f(a), f(b)), \max(f(a), f(b))] \quad (7)$$

When the mapping is for n input variables, i.e., $y = f(x_1, x_2, \ldots, x_n)$, and each input variable is described by an interval, say $I_{i\lambda}$ at a specific λ-cut, where $I_{i\lambda} = [a_i, b_i]$, $i = 1, 2, \ldots, n$, then values of interval function representing output fuzzy set B at a particular value of λ, is given by

$$\begin{aligned} B_\lambda &= f(I_{1\lambda}, I_{2\lambda}, \ldots, I_{n\lambda}) \\ &= [\min_j (f(c_j)), \max_j (f(c_j))], \quad j = 1,2,\ldots,N \end{aligned} \quad (8)$$

where $N = 2^n$, and c_j represents all possible combinations of input interval variables, i.e., they are vertices of input space in the n-dimensional Cartesian region.

Kandil [14] reported that the ambiguities in the determination of plastic strain ranges in TMF can cause variations up to 30% in the estimated plastic strain range. A rational approach would be to treat the strain range as a fuzzy variable. Therefore the partitioned inelastic strain-ranges (namely, $\Delta\varepsilon_{PP}$, $\Delta\varepsilon_{CC}$, $\Delta\varepsilon_{PC}$ and $\Delta\varepsilon_{CP}$) are also fuzzy sets. In the present study, a triangular membership function with 30% variation in either side is assumed for the fuzzy sets for the partitioned inelastic strain-ranges. The

fatigue coefficients A_{ij} and the fatigue exponents C_{ij} are considered as random variables to consider the variations in the micro-structural properties of the material of the piping component. The fatigue coefficients are assumed to follow a lognormal distribution with a coefficient of variation of 0.05 and the fatigue exponents are assumed to follow a normal distribution with a coefficient of variation of 0.05 [16]. The limit state function used is $N_f - N$, where N_f is the number of load cycles to failure (a fuzzy-random variable) obtained using the proposed approach and N is the applied load cycles (considered as deterministic in the present study). The λ-cut levels are taken as 0^+, 0.2, 0.4, 0.6, 0.8 and 1.0. For each λ-cut level, there are two values for each partitioned inelastic strain-range. For different combination of values of the strain range for a given λ-cut level, probabilistic analysis of the fatigue life is carried out using Monte Carlo simulation (MCS) technique with one million simulation cycles, and the λ-cut of fuzzy set for failure probability (P_F) is determined.

4. Example

The main steam pipe of a thermal power plant that had been operating for about 130000 hrs at a temperature of 538°C and a pressure of 148 atm is considered [16]. The material of the pipe is 2.25Cr-1 Mo steel. The values of material fatigue coefficients, material fatigue exponents, strain ranges and the experimentally determined TMF life ($(N_f)_{expt}$ in load cycles) are taken

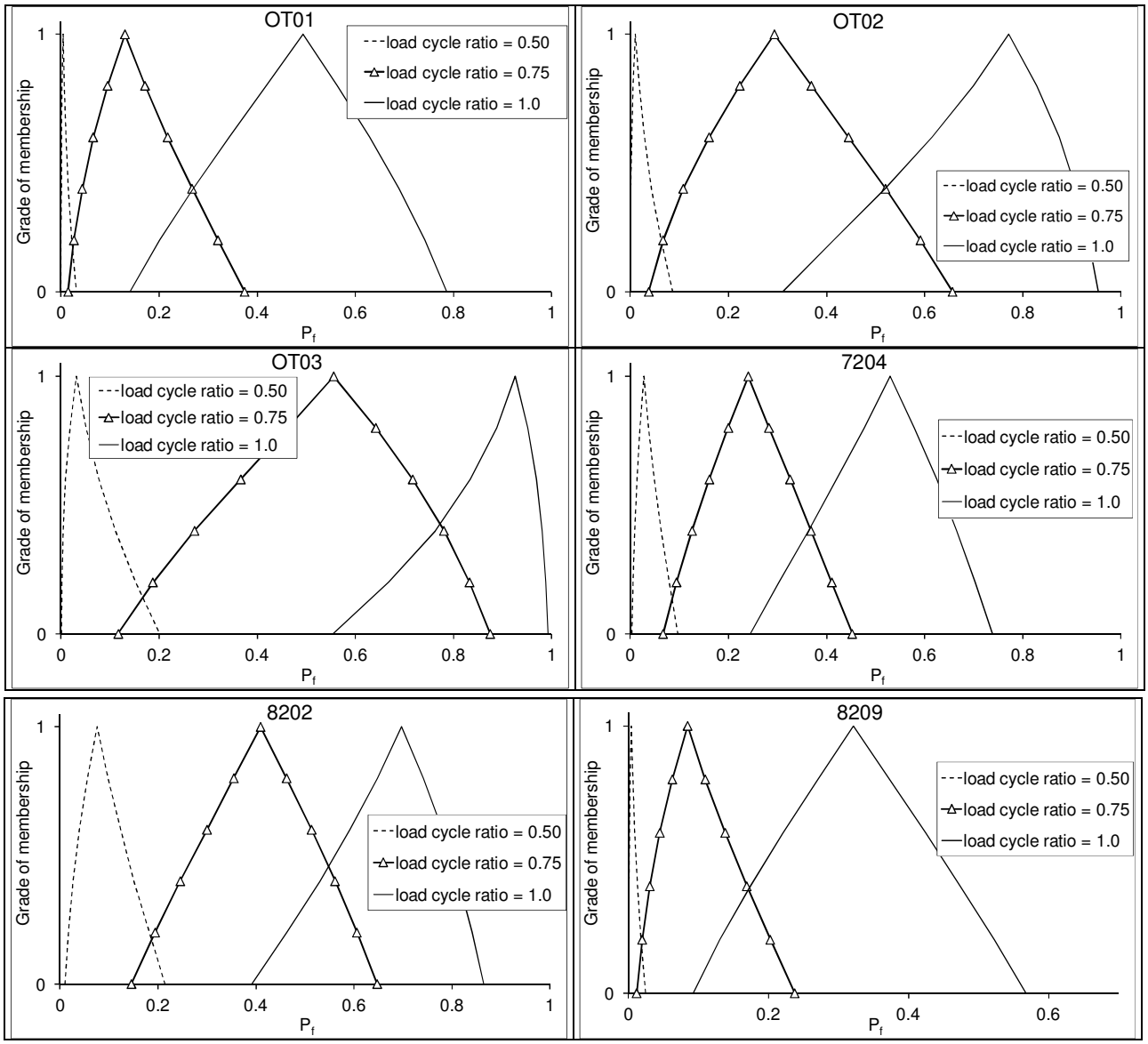

Fig. 1 Fuzzy sets of failure probability for different values of load cycle ratio (applied load cycles/ experimentally observed load cycles to failure) for the test specimens considered

Table 2 Elastic- and inelastic- strain ranges and the number of load cycles to failure from experimental investigations [16] and using SRP model for different specimens of the 2.25Cr-1Mo Steel steam pipe considered

specimen	$\Delta\varepsilon_{el}$	$\Delta\varepsilon_{in}$	$\Delta\varepsilon_{el}/\Delta\varepsilon_{in}$	$(N_f)_{expt}$	$(N_f)_{SRP}$	$(N_f)_{expt}/(N_f)_{SRP}$
OT03	0.237	0.763	0.31	853	629	1.36
8202	0.231	0.569	0.41	1667	1369	1.22
OT02	0.226	0.574	0.39	998	850	1.17
7204	0.226	0.324	0.70	2248	2188	1.03
OT01	0.212	0.338	0.63	1478	1506	0.98
8209	0.263	0.737	0.36	947	1104	0.86

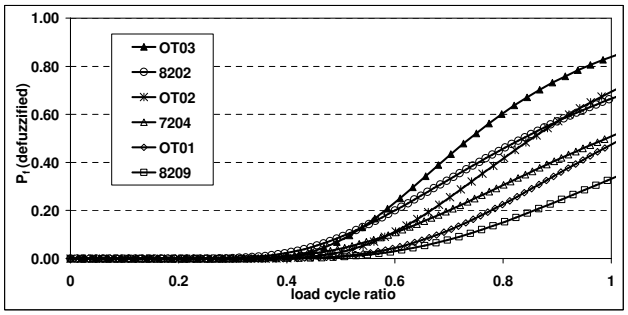

Fig. 2 Defuzzified values of failure probability for different test specimens made of 2.25Cr-1Mo steel (load cycle ratio = applied load cycles/ experimentally observed load cycles to failure)

from [16]. The TMF lives, deterministically determined using the SRP model ($(N_f)_{SRP}$) for these specimens are given in Table 2, along with the experimental values. The value of $(N_f)_{expt}/(N_f)_{SRP}$ is different for the different test specimens considered (see Table 2), and the variations in the values of $(N_f)_{expt}/(N_f)_{SRP}$ suggests that there is a need to consider the modeling error as a random variable. However, the modeling error is not considered in the present study.

The fuzzy sets for failure probability (P_F) are determined for different applied load cycles. The fuzzy sets for failure probability corresponding to different values of load cycle ratio (defined as the ratio of applied load cycles to experimentally observed load cycles to failure) for the test specimens considered are shown in Fig. 1. From this figure, it is noted that interval lengths of fuzzy sets of P_F at a given l-cut level increase with increase in loading cycles, resulting in increase in uncertainty about P_F. The defuzzified values of failure probability for different specimens considered are shown in Fig. 2. It is noted that the failure probabilities for different specimens shows the same ordering as one would have inferred from the results of deterministic study. By carrying out a complete probabilistic analysis, while it is possible to obtain the bounds on failure probability, it may be computationally expensive to obtain the probability distribution for the failure probability. But from the resulting fuzzy set for failure probability obtained from a fuzzy-probabilistic analysis, the bounds of failure probability for different λ-cut levels can be identified. This will be more useful in decision-making since one can set parametric confidence limits on failure probability by considering an appropriate λ-cut level. The proposed procedure will help in rationally taking into account various uncertainties while designing the components with known/acceptable levels of safety specified either in codes or by learned bodies (AERB codes/NUREG).

5. Summary

The safety assessment of a nuclear power plant piping component against thermo-mechanical fatigue with number of cycles, by treating the relevant uncertain variables as random or fuzzy depending upon the source of uncertainty, is presented. The fuzzy failure probabilities are computed using the procedure developed at CSIR-SERC, combining the vertex method with Monte Carlo simulation technique. The strain range partitioning approach, which is the general approach employed for continuum response in safe-life, finite-life region i.e., the low cycle fatigue region with stabilized cyclic stress-strain constants, is used in the safety assessment for determining the thermo-mechanical fatigue life. An example of a main steam piping of an operating thermal power plant is considered for safety assessment. From the results obtained, it is noted that the fuzzy-probabilistic approach presented shows promise for safety assessment of nuclear power plant pipelines, and will be useful for making decisions regarding in-service inspections.

Acknowledgements

This paper is being published with the kind permission of the Director, CSIR-Structural Engineering Research Centre, Chennai, India.

References

1. Helton, J.C. and Oberkampf, W.L. (2004), Alternative representations of epistemic uncertainty, Reliability Engineering and System Safety, 85, pp. 1-10
2. Nagesha, A., Valsan, M., Kannan, R., Bhanu Sankara Rao, K. and Mannan, S.L., "Influence of temperature on the low cycle fatigue behaviour of modified 9Cr-1Mo ferritic steel", International Journal of Fatigue, 24, 1285-1293, 2002.
3. Lin, C.K. and Pai, Y.L., "Low-cycle fatigue of austempered ductile irons at various strain ratios", International Journal of Fatigue, 21, pp. 45-54, 1999.
4. Zhuang, W.Z. and Swansson, N.S., "Thermo-mechanical fatigue life prediction: a critical review", DSTO Aeronautical and Maritime Research Laboratory, Australia, 1998.
5. Manson, S., Halford, G. and Hirschberg, M., "Creep-fatigue analysis by strain-range partitioning", symposium on design for elevated temperature environment, ASME, New York, pp. 12-28, 1971.
6. Manson, S., "The challenge to unify treatment of high temperature fatigue – a partisan proposal based on strain-range partitioning", Fatigue at elevated temperatures, STP 520, Philadelphia, ASTM, pp. 744-782, 1973.
7. Hoffelner, W., Melton, K.L. and Wuthrich, C., "On life time predictions with the strain range partitioning method", Fatigue & Fracture of Engineering Materials & Structures, 6(1), pp. 77–87, 1983.
8. Halford, G. and Nachtigall, A., "The strain-range partitioning behavior of an advanced gas turbine disk alloy AF2-1DA", Paper No. 79-1192, presented at the AIAA/SAE/ASME 15th Joint propulsion Conference, 18-20 June 1979.
9. Bernstein, H., "An evaluation of four creep-fatigue models for a nickel-base superalloy, Low-Cycle Fatigue and Life Prediction, ASTM STP 770", C. Amzallag, B. Leis, and P. Rabbe, eds., American Society for Testing and Materials, pp. 105-134, 1982.
10. Halford, G.R., Manson, S.S., "Life prediction of thermal-mechanical fatigue using strain range partitioning, Thermal Fatigue of Materials and Components", (eds.) D.A. Spera, D.F. Mowbray, ASTM STP 612, pp 239–254, 1976.
11. Nitta, A. and Kuwabara, K., "Thermal-mechanical fatigue failure and life prediction", High Temperature Creep-Fatigue, Ohtani, R., Ohnami, M. and Inoue, T., eds., Elsevier Applied Science, pp. 203-222, 1988.
12. Anoop, M. B., Balaji Rao, K. and Lakshmanan, N., "Safety assessment of austenitic steel nuclear power plant pipelines against stress corrosion cracking in the presence of hybrid uncertainties", International Journal of Pressure Vessels and Piping, 85(4), pp. 238–47, 2008.
13. Dong, W. and Shah, H., "Vertex method for computing functions of fuzzy variables", Fuzzy Sets and Systems, 24, pp. 65-78, 1987.
14. Kandil, F.A., "Potential ambiguity in the determination of the plastic strain range component in LCF testing", International Journal of Fatigue, 21(10), pp. 1013–1018, 1999.
15. Kandarpa, S., Spencer, B.F. and Kirkner, D.J., "Reliability analysis of structural components utilizing the strain-life method", Engineering Fracture Mechanics, 53(5), pp. 761-774, 1996.
16. Saltsman, J. and Halford, G., "Ability of the total strain version of strain-range partitioning to characterise thermo-mechanical fatigue behavior", NASA TM – 4556, 1994.
17. Hirschberg, P., "Materials reliability program: operating experience regarding thermal fatigue of piping connected to PWR reactor coolant systems (MRP-85)", Revision 1 to 1001006 (MRP-25). EPRI, Palo Alto, CA: 2003. 1007761.

SRESA JOURNAL SUBSCRIPTION FORM

Subscriber Information (Individual)

Title	First Name	Middle Name	Last Name
_____	_____	_____	_____

Street Address Line 1	Street Address line 2
_____	_____

City	State/Province	Postal Code	Country
_____	_____	_____	_____

Work Phone	Home Phone	E-mail address
_____	_____	_____

Subscriber Information (Institution)

Name of Institution/ Library _____

Name and Designation of Authority for Correspondence _____

Address of the Institution/Library _____

Subscription Rates

	Subscription Quantity	Rate	Total
Annual Subscription (in India)	_____	Rs. 15, 000	_____
(Abroad)	_____	$ 500	_____
	_____		_____
	_____		_____

Payment mode (please mark)

Cheque ☐ Credit Card ☐ Master Card ☐ Visa ☐ Online Banking ☐ Cash ☐ De mand Draft ☐

Credit card Number _____

Credit Card Holders Name _____

Credit Card Holde _____

Guidelines for Preparing the Manuscript

A softcopy of the complete manuscript should be sent to the Chief-Editors by email at the address: editor@sresa.org.in. The manuscript should be prepared using 'Times New Roman' 12 font size in double spacing, on an A-4 size paper. The illustrations and tables should not be embedded in the text. Only the location of the illustrations and tables should be indicated in the text by giving the illustration / table number and caption.

The broad structure of the paper should be as follows: a) Title of the paper – preferably crisp and such that it can be accommodated in one or maximum two lines with font size of 14 b) Name and affiliation of the author(s), an abstract of the paper in ~ 100 words giving brief overview of the paper and d) Five key words which indicates broad subject category of the paper. The second page of the paper should start with the title followed by the Introduction

A complete postal address should be given for all the authors along with their email addresses. By default the first author will be assumed to be the corresponding author. However, if the first author is not the corresponding author it will be indicated specifically by putting a star superscript at the end of surname of the author.

The authors should note that the final manuscript will be having double column formatting, hence, the size of the illustration, mathematical equations and figures should be prepared accordingly.

All the figures and tables should be supplied in separate files along with the manuscript giving the figure / table captions. The figure and table should be legible and should have minimum formatting. The text used in the figures and tables should be such that after 30% reduction also it should be legible and should not reduced to less than font 9.

Last section of the paper should be on list of references. The reference should be quoted in the text using square bracket like '[1]' in a chronological order. The reference style should be as follow:

1. Pecht M., Das D, and Varde P.V., "Physics-of-Failure Method for Reliability Prediction of Electronic Components", Reliability Engineering and System Safety, Vol 35, No. 2, pp. 232- 234, 2011.

After submitting the manuscript, it is expected that reviews will take about three months; hence, no communication is necessary to check the status of the manuscript during this period. Once, the review work is completed, comments, will be communicated to the author.

After receipt of the revised manuscript the author will be communicated of the final decision regarding final acceptance. For the accepted manuscript the author will be required to fill the copy right form. The copy right form and other support documents can be down loaded from the SRESA website: http://www.sresa.org.in

Authors interested in submitting the manuscript for publication in the journal may send their manuscripts to the following address:

Society for Reliability and Safety
RN 68, Dhruva Complex
Bhabha Atomic Research Centre,
Mumbai – 400 085 (India)
e-mail : editor@sresa.org.in

The Journal is published on quarterly basis, i.e. Four Issues per annum. Annual Institutional Subscription Rate for SAARC countries is Indian Rupees Ten Thousand (Rs. 10,000/-) inclusive of all taxes. Price includes postage and insurance and subject to change without notice. For All other countries the annual subscription rate is US dollar 500 ($500). This includes all taxes, insurance and postage.

Subscription Request can be sent to SRESA Secretariat (please visit the SRESA website for details)

SRESA's International Journal of

Life Cycle Reliability and Safety Engineering

Contents

Vol.3 **Issue No.2** **April-March 2014** **ISSN – 2250 0820**

Optimal Design of Monitoring Systems for Risk Reduction and Operation Benefits
Sebastian Thöns, Michael Havbro Faber, Werner Rücker (Denmark).....1

Massive Shear Wall Testing for Nuclear Industry
Adrian Bekö, Helmut Wenzel, Peter Rosko (Austria).....11

Ageing Behaviour of Structural Components for Integrated Lifetime Assessment and Asset Management
Robert Veit-Egerer, Helmut Wenzel, Rui Lima (Austria) 22

An Approach for Reliability Based Control of Post-Tensioned Containment Structure
Alexander ILIEV, Marin KOSTOV, Anton ANDONOV (Bulgaria) 30

Time Dependent PSA of Nuclear Power Plants Under Seismic Events
M. Hari Prasad, P. N. Dubey, Gopika Vinod, G. R. Reddy and R.K. Singh (India).....41

Probabilistic Failure Assessment of PWR Nuclear Power Plant Piping Components against Erosion-Corrosion
Jiboy Jose, K. Balaji Rao, M. B. Anoop, Gopika Vinod, H. S. Kushwaha (India) 48